EVALUATION OF GROUND COUPLED HEAT PUMPS FOR THE STATE OF WISCONSIN

by

Jonathan J. Giardina

A thesis submitted in partial fulfillment of

the requirements for the degree of

MASTERS OF SCIENCE

(MECHANICAL ENGINEERING)

at the

UNIVERSITY OF WISCONSIN-MADISON

1995

TABLE OF CONTENTS

CHAPTER
ONE

INTRODUCTION

Consumer demand for electricity, and the emissions associated with its generation, will continue to rise steadily into the future if the current level of technology is maintained (WCDSR #2, 1994). Residential heating and cooling, which accounts for more than 25% of the nations total electrical energy consumption, holds potential for large energy savings. The Department of Energy (DOE) is promoting ground coupled heat pumps (GCHP) as an alternative to conventional heating and cooling systems because of their ability to operate efficiently in most U.S. climates (U.S. Dept. of Energy, 1994). This efficiency is due to the use of ground temperatures which do not experience the extremes of ambient air temperatures used by air source heat pumps. The high electrical efficiency and use of "clean" geothermal energy were noted as a tremendous opportunity to reduce energy use and emission levels. The DOE program calculated that over the equipment lifetime of 20 years, every 100000 units will save over 37.5 trillion Btu of energy and reduce emissions by 2.18 million metric tons of carbon equivalents.

Customers may find the prospect of conserving energy and reducing pollutants enticing, however the decision to install a GCHP would probably be one of economics. For instance, a customer switching from electric resistance heating to a GCHP would save money with each electric bill. However, the initial cost of a GCHP system is usually thousands of dollars more than a conventional heating and cooling system due the added expense of coupling the system to the ground. The customer saves money over a given period of time if the energy savings are large enough to offset the increase in installation costs. Although GCHP are always economically competitive with

resistance heat, current natural gas and electric rates in most locations are such that a GCHP is not a profitable economic alternative to a natural gas furnace. Therefore, GCHP markets have usually been in regions with a low penetration of natural gas service. Wisconsin, which is currently considering an aggressive GCHP program, has no natural gas service for approximately 33% of its 1.81 million residential electric customers.

1.1 Literature Review

In the past, GCHP systems have been modeled using bin analysis methods. Two bin method programs which are widely used include a program from Oklahoma State University (OSU) and a program from Water Furnace, a major GCHP manufacturer. The OSU program, called Closed Loop Ground Source Design (CLGS), uses two heat pump operating points to model the heat pump performance. The Water Furnace program, a programmed Excel spread sheet, has its performance models hidden from the user. Simple approximations are used in both of these programs to model the water temperature entering the GCHP. The two programs also have sections for buried heat exchanger sizing, each based on the line-source method (Hart, 1986). Field installations have shown that this method provides safe loop length estimates, over predicting the heat exchanger length required to return a desired minimum entering water temperature. Desuperheater operation, an attachment to the GCHP which allows it to heat water, is roughly approximated by each of these methods. These models are popular because they are fast and easy to use, and the buried heat exchanger sizing programs can approximate the necessary design for a number of loop configurations quickly.

A transient analysis, which allows house loads, heat pump operation, and desuperheater operation to be modeled with more complexity, will also allow for a more detailed modeling of the water temperatures entering the GCHP. A finite difference model of the buried heat exchanger allows for the capacitance of the soil to be captured, enabling soil and heat exchanger fluid temperatures to change with time. Several models were found in the literature that used this method to varying

degrees of complexity. A model from Oak Ridge National Lab (ORNL) for the ground heat transfer was used as the basis for the model used in this study (Mei, 1986). ORNL modeled a buried pipe surrounded by a cylinder of soil, where heat transfer could occur both radially and circumferentially. The pipe was broken into sections along its length, and uniform soil properties were assumed for the entire soil field. Temperatures at the outer radius of the cylinder varied, were assumed undisturbed by the heat transfer from the pipe, and were given a realistic temperature profile that changed with time and with depth. There was no moisture migration or soil freezing accounted for in the model. The ORNL model is an excellent base for a transient analysis since it is able to model the capacitance of the soil and return a water temperature leaving the pipe for each transient simulation time step.

1.2 Project Scope

This project will investigate several aspects of the GCHP market in Wisconsin using computer modeling techniques. TRNSYS, a transient simulation program, will be used to model GCHP and conventional heating and cooling systems. The ground heat exchanger will be modeled using a finite difference approach based on the model by ORNL, where the soil around the pipe is divided into a grid nodes, each with a temperature and thermal capacitance. Desuperheater operation will be modeled using a stratified tank model that uses a hot water load profile generated with WATSIM, a residential hot water load generating program (EPRI, 1992). The house model used to generate loads for the heating and cooling equipment will consist of a single thermal capacitance and overall heat transfer coefficient, with loads driven by weather data containing an hourly account of the ambient air temperature and the global radiation level.

The new TRNSYS models will add in several ways to the current array of GCHP energy analysis programs available. The biggest advantage of the transient simulation is that it will allow loads and energy consumption to be tracked with time, allowing for the investigation of on and off peak energy use. The transient simulation will allow for the desuperheater to be modeled more accurately by

capturing the coincidence of heat pump operation and hot water demand, modeling the dependence of desuperheater performance on the coldest tank water temperature, and calculating tank losses. It will also add to the currently available programs by allowing performance variations such as thermostat control strategies, desuperheater configurations, heat exchanger length, heat exchanger depth, soil type, and location to be investigated.

The models developed for this project will be used to investigate several different aspects of GCHP performance. Weather data from two Wisconsin locations, Madison and Eau Claire, will be used to create loads on the house model which has a design heating load of 50000 Btu/hr. The heating and cooling systems used in the comparison will include resistance heating, natural gas furnace, vapor compression air conditioning, air source heat pump, GCHP, GCHP with a desuperheater, and a well source heat pump system with water heating accessory. The total energy consumption, peak power, life cycle savings, and avoided costs of different heating and cooling systems will be compared.

Many different sizes of GCHP are available for a house with a design winter heating load of 50000 Btu/hr. This report will compare the life cycle savings and avoided costs of a 5.83, 4.75, 3.75, 3.33, and 2.83 ton GCHP, using a resistance heated house with a 3.5 ton air conditioner as the base system. This comparison will provide information on the best choices for the customer and the utility. Performance in Madison and Eau Claire will be compared to evaluate whether location has any effect on the relative LCS of the systems.

High installation costs associated with the buried heat exchanger are the single largest obstacle to the wide spread installation of GCHP. The effect of installation cost will be investigated in two ways. In the first approach, simulations with a 3.33 ton GCHP will be performed for heat exchanger lengths ranging from 1000 to 3000 feet. Life cycle savings vs. heat exchanger length will be plotted for this system to identify a possible strategy for sizing the heat exchanger for the best life cycle savings. For the second approach, different buried heat exchanger installation costs will be

investigated to compare how a change in installation cost effects the GCHP life cycle savings. A 4.75 and 3.33 ton GCHP will be run with a set length, with only the costs of installation being varied.

The effect of house size on GCHP performance will be investigated using a 5.83 and 3.75 ton GCHP, using resistance heat with a 3.5 ton air conditioner as the base system. The house sizes tested will have 60, 50, and 40 MBtu/hr design heating loads for a Madison location. This study is looking to see how the LCS and avoided costs of the different systems compare in differently sized houses.

CHAPTER
TWO

HEAT PUMP SYSTEMS

This section discusses the vapor-compression cycle used by the heat pump, the advantages of ground coupled heat pumps, and the options available for coupling the heat pump to the ground.

2.1 Description of the Heat Pump Cycle

Heat pumps use the vapor compression cycle shown in Figure 2.1 on temperature-entropy coordinates. Refrigerant enters the compressor at point A, where it is compressed to a higher

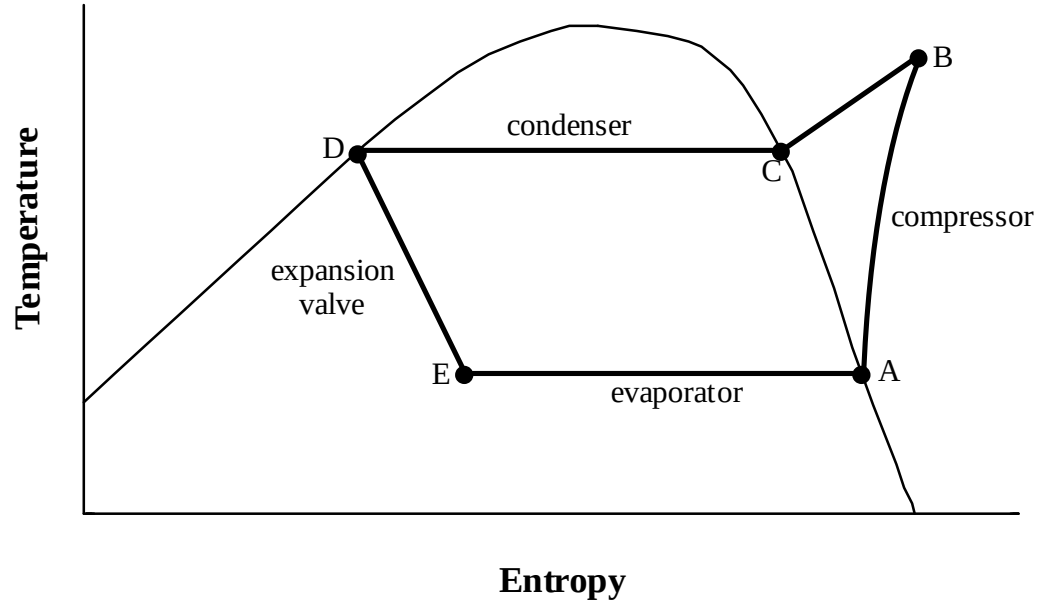

Figure 2.1 Temperature-Entropy diagram of vapor compression cycle

temperature and pressure, point B. In the condenser, energy is removed from the refrigerant with a cool external fluid, causing it to cool to point C and condense to point D. At point D, the refrigerant enters an expansion valve which decreases the pressure and temperature. At point E, low temperature refrigerant enters the evaporator, evaporating as it removes energy from a warmer external fluid. It then reenters point A again and repeats the cycle.

The vapor-compression cycle can be used to both heat and cool. During cooling, the evaporator coil cools and removes moisture from the indoor air stream, $\dot{Q}_{evap}$. The condenser is located outdoors and rejects $\dot{Q}_{cond}$ (equal to $\dot{Q}_{evap} + \dot{W}_{comp}$) to the surroundings. The equipment arrangement for cooling in shown in Figure 2.2.

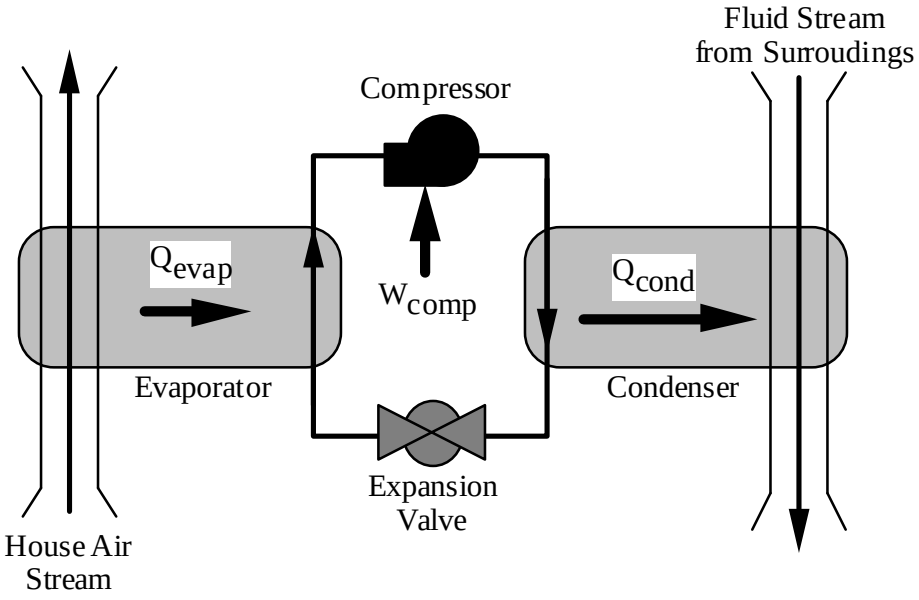

Figure 2.2 Vapor compression cooling cycle arrangement.

For heating, the evaporator is located outdoors where it absorbs $\dot{Q}_{evap}$ from the surroundings. The condenser, located indoors, releases $\dot{Q}_{cond}$ (equal to $\dot{Q}_{evap} + \dot{W}_{comp}$) to the indoor air stream. This arrangement is shown in Figure 2.3.

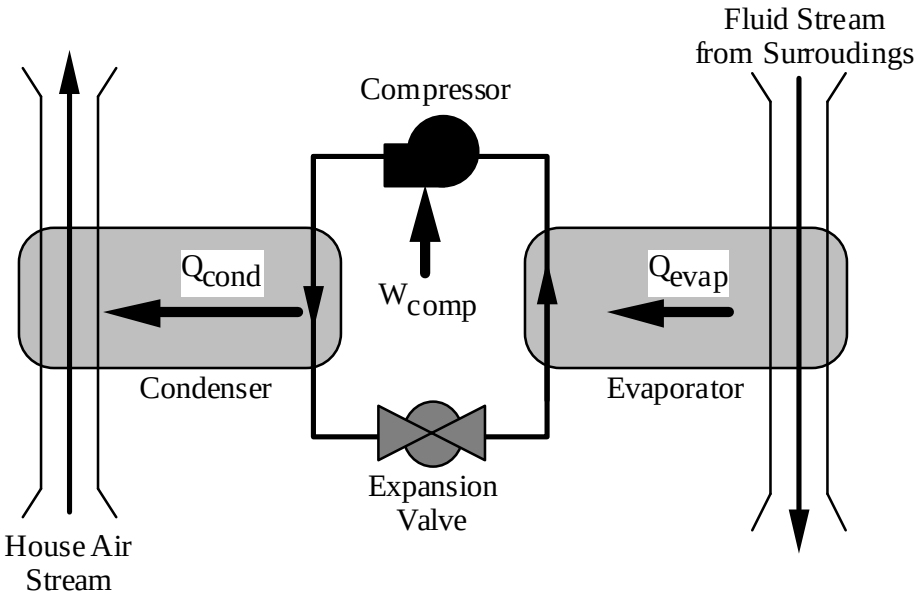

Figure 2.3 Vapor compression heating cycle arrangement.

When used for heating, the performance of the vapor compression cycle is rated with a coefficient of performance (COP), and when cooling, is rated with an energy efficiency ratio (EER). These performance ratings are given in equations 2.1 and 2.2.

$$\mathrm{COP} = \frac{\dot{Q}_{cond}\ [\mathrm{Btu/hr}]}{\dot{W}_{comp}\ [\mathrm{Btu/hr}]} \tag{2.1}$$

$$\mathrm{EER} = \frac{\dot{Q}_{evap}\ [\mathrm{Btu/hr}]}{\dot{W}_{comp}\ [\mathrm{kW}]} \tag{2.2}$$

Heat pumps are efficient heaters when compared to the conventional electric heating systems which use resistance coils to heat the air. With a resistance heating coil, one unit of electric energy is turned into one unit of heat supplied to the room, resulting in a COP of 1.0. A heat pump operating with a COP of 3.0 can supply a total of 1.0 units of heat using only 0.33 units of electrical energy to run the compressor. The other 0.66 units of energy were absorbed by the evaporator from the surroundings.

The performance of the vapor compression cycle is sensitive to the evaporator and condenser temperatures. A decrease in evaporator temperature, or an increase in condenser temperature, decreases the cycle COP. This can be seen using the optimal case of the Carnot refrigeration cycle. The Carnot refrigeration cycle is shown in Figure 2.4, where T_H is the condenser temperature and T_L is the evaporator temperature. Equation 2.3 is used to calculate the Carnot COP.

$$COP = \frac{T_H}{T_H - T_C} \tag{2.3}$$

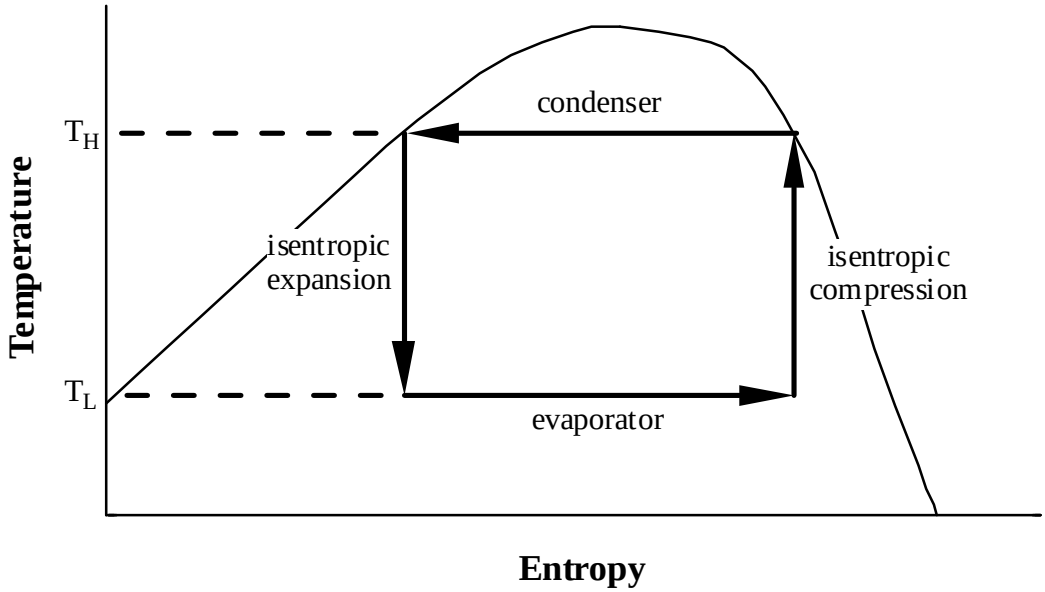

Figure 2.4 Carnot refrigeration cycle

If the temperature difference between the evaporator and condenser increases, the value of the numerator will increase, thus the COP of the system will fall. For a real system, this drop in COP is tied to the rapid decrease in refrigerant density entering the compressor as temperatures decrease. Since the compressor is approximately a constant volume device, this decrease in density means that the mass flow rate of refrigerant through the entire system has decreased, decreasing both the energy input by the compressor and the rate at which energy is transported from the evaporator to the condenser.

2.2 Air Source Heat Pump

The most commonly installed heat pump in residential applications is the air source heat pump (ASHP). This means that the heat pump uses the surrounding ambient air as an energy source or sink. When ambient temperatures do not drop below 40 or 50°F, the cycle operates with a capacity and COP large enough to provide substantial energy savings compared to an electric resistance heated house. If the ambient air temperature drops below 30°F, the low evaporator temperature would result in a decrease of the heat pump cycle COP and capacity. Evaporator temperatures below freezing promote the build up of frost on the evaporator surfaces, decreasing its effectiveness, and further decreasing the cycle COP and capacity. The frost is removed using a defrost cycle, where the system is run as an air conditioner, forcing hot refrigerant through the frozen outdoor coils. These defrost cycles, which must be run periodically, reduce the average COP of the heat pump system in two ways. First, the energy

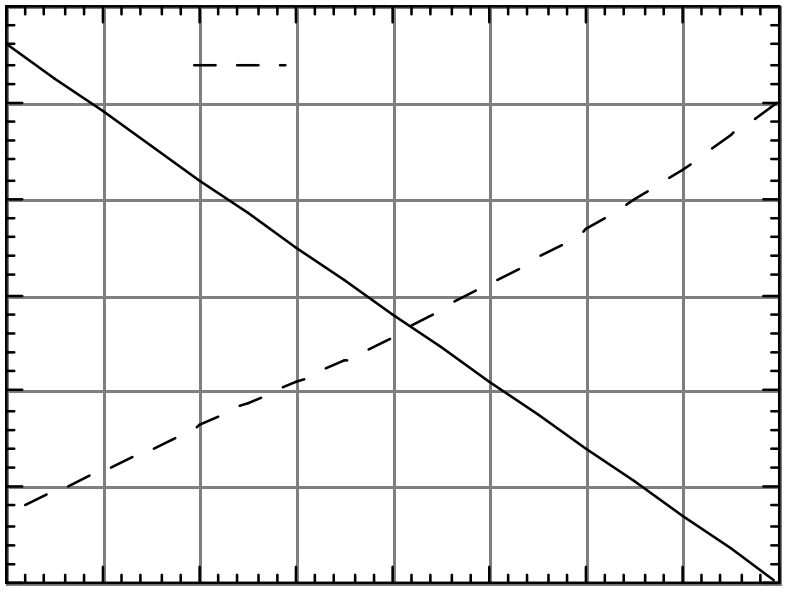

Figure 2.5 House heating load and ASHP heating capacity vs. $T_{ambient}$

used to melt the frost is lost to the surroundings. Second, since the defrost cycle is an air conditioning cycle, the indoor space is being cooled. Resistance heat must be used to replace the energy removed, maintaining the temperature of the house. These two effects will reduce the COP of the system so drastically that most ASHPs do not operate when outdoor air temperatures are below 20°F.

ASHPs installed in homes are not sized to meet all of the heating load. As outdoor temperatures drop and the heating loads increase, the COP and capacity of the heat pump decrease due to lower evaporator temperatures, as shown in Figure 2.5. With the heat pump only meeting from 0 to 20% of the load during the worst winter conditions, auxiliary heating is required. Auxiliary heating is usually supplied in the form of staged resistance heat, coming on when the heat pump cannot meet the entire heating load alone. When all of the auxiliary heat stages are running, the overall COP of the heating system decreases, approaching 1.0. This offsets the efficiency advantage that the heat pump has at more reasonable ambient temperatures.

2.3 Ground Coupled Heat Pump Advantages

While the ASHP has proven to be a popular heating alternative in the southern states, their poor performance in low ambient air temperatures has limited sales in the northern states The low winter ambient temperatures cause severe decreases in system COP, increasing the reliance on expensive auxiliary resistance heat. Furthermore, since ASHPs use the same ambient air during the summer as a vapor compression air conditioner, they provide no peak demand reduction. Utilities want to reduce summer peak demand, so they are not likely to encourage the installation of ASHP units. Heat pump technology would benefit from the elimination of the defrost cycle, increasing the average COP during heating. Heat pump cycles could also be improved by utilizing more reasonable source and sink temperatures

which would reduce the summer peak demand and auxiliary heat operation. Ground coupled heat pumps (GCHP) provide these performance advantages.

The GCHP uses the temperature of the earth to maintain better evaporator and condenser temperatures during both the cooling and heating cycles. The temperature of the earth does not experience the extremes in temperature that the ambient air does. In fact, at reasonable depths the ground temperature maintains an almost constant value, T_{mean}, throughout the year. During heating, the higher evaporator temperature means better cycle COP and heating capacity, resulting in less reliance on auxiliary heating. Also, since no heat exchanger surface is exposed to ambient air, no defrost cycle is needed.

Another benefit of the GCHP is that the entire system, except for the buried heat exchanger, can be located indoors. This reduces the wear and tear the system experiences, giving it a life expectancy of 20 years. ASHPs, which locate an expensive heat exchanger and compressor outside, have a life expectancy of only 10 years (Golish, 1994).

Another advantage the GCHP has over the ASHP is the capability to meet some of the hot water load through the use of a desuperheater. The desuperheater, a heat exchanger located immediately after the compressor, uses the hottest refrigerant of the vapor compression cycle, the superheated vapor from point B to C in Figure 2.1, to exchange energy with tank water. The desuperheater is named because it cools the superheated refrigerant toward the liquid-vapor dome at point C. Water heated with the desuperheater utilizes the superior COP of the heat pump, whereas water heated with resistance coils has a COP of 1.0. Since the cost of heating water can be around 20 to 30% of the annual heating and cooling energy bill, the savings generated by the desuperheater can be significant, paying for itself in a matter of years.

During the cooling season, some of the energy to be rejected by the condenser as waste heat is sent to the hot water tank. In effect, the water is being heated for free. During the winter, operation of the desuperheater reduces the heating capacity of the heat pump by diverting energy to the hot water tank that would have gone to the house. Thermostats monitor when the full heat pump capacity is needed to heat the house, shutting down desuperheater operation.

2.4 The Ground as Source and Sink

The energy of the earth is tapped with a buried heat exchanger or through the use of well water. The well water system, or well source heat pump, draws water from an underground water table, uses it to extract or reject energy, and then returns it to the surface. It has the advantage of being inexpensive to install when the property already has an existing well. It also has the advantage of operating at a nearly constant water temperature throughout the year. This water temperature, which is around 50°F in Wisconsin, gives excellent performance for both heating and cooling.

A closed loop heat exchanger circulates an antifreeze solution through a circuit of buried polyethylene or polybutylene pipes. Turbulent flow is maintained to encourage high heat transfer coefficients. The antifreeze passes through the heat pump heat exchanger (evaporator or condenser) where it delivers or absorbs energy. The fluid then continues through the pipe circuit absorbing or rejecting energy to the ground. The closed loop ground heat exchanger has less ideal operating temperatures than the well source. During operation, fluid temperatures from a heat exchanger at a depth of 6 feet in Wisconsin can vary from 25 °F in the winter to 80°F in the summer, causing the efficiency of the GCHP to decrease. The buried heat exchangers are also more expensive to install than the well source. However, they may be the only choice for areas where ground water is not abundant, proper drainage is not available, or local regulations prohibit the use of well water.

Closed loops come in three varieties: horizontal, vertical, and pond loops. A pond loop consists of a series of coiled plastic tubes placed on the bottom of a body of water. Anti-freeze is circulated from the heat pump to the submerged coils which use the lake water as an energy source or sink. Pond loops are used when a pond is located close to the residence to avoid digging long trenches to and from the pond. Installation costs for pond loops are usually the lowest of the buried heat exchangers (Hoover, 1994).

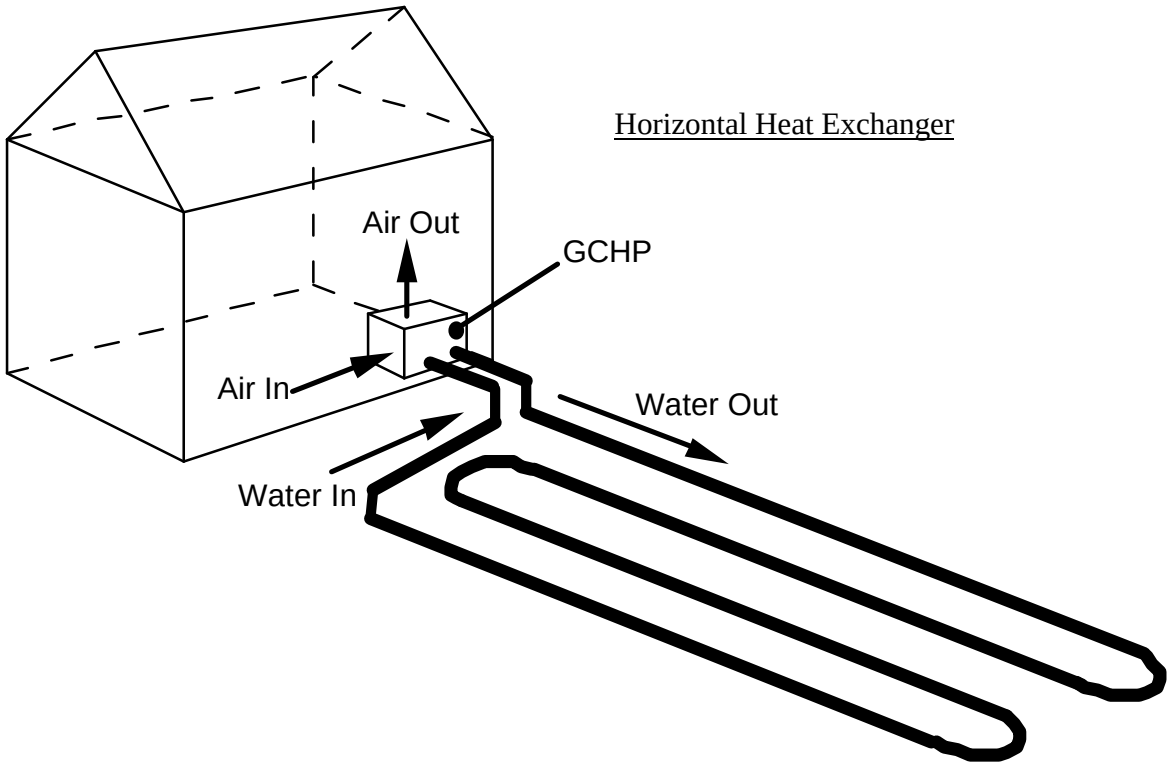

Figure 2.6 Horizontal closed loop ground coupled heat pump

The horizontal closed loop heat exchanger consists of pipes that are buried in horizontal trenches in the ground. The pipe depth can be from 3 to 8 feet depending on the geographic location. The installation of the horizontal heat exchanger requires a large amount of space, since loop lengths will often consist of a few thousand feet of pipe. Figure 2.6 is a simplified picture of a horizontal heat exchanger. In order to reduce the installation cost of horizontal heat exchangers, several pipes can be placed in one trench. Arrangements of two, four, six,

and even nine pipes per trench are currently being installed by contractors. Figure 2.7 shows cross-sectional views of different multiple pipe configurations (OSU, 1988).

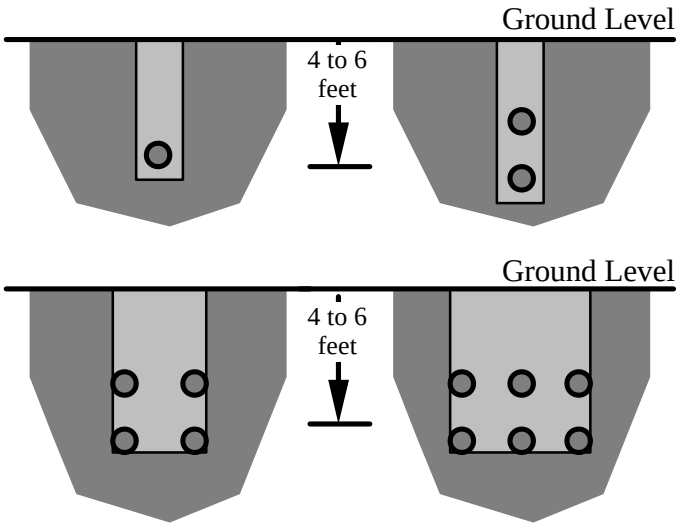

Figure 2.7 Cross sections of multiple pipe per trench formations

Pipes placed in close proximity will thermally interfere with one another, reducing the heat transfer per lineal foot of pipe. However, the cost of the installation is not driven by the heat transfer per lineal foot of *pipe*, but by heat transfer per lineal foot of *trench*, since the cost per lineal foot of pipe is much lower than the cost per lineal foot of trench. Increasing the density of pipes per trench will increase the effectiveness of the trench, reducing the total length of trench needed.

The most expensive closed loop installation is the vertical heat exchanger. Vertical heat exchangers are installed where land space is limited and a water well with adequate drainage is not available. A vertical heat exchanger consists of a series of vertically bored holes, each containing two pipes attached at the bottom by a U-bend. This configuration is shown in Figure 2.8. Anti-freeze flows from the heat pump down into the pipe where it absorbs energy during the winter and rejects energy during the summer.

Horizontal and vertical loops come in both parallel and series configurations. A series loop has the entire fluid flow passing through one pipe. Figure 2.6 shows a horizontal loop in a series arrangement. A parallel system divides the total flow into multiple branches with a header system. Figure 2.8 shows a vertical loop in a parallel arrangement. For a series system to handle the entire fluid flow at a reasonable head loss, a larger diameter pipe, on the order of 1.5 inches, must be used. This larger diameter pipe has the advantage of encouraging a higher heat transfer per lineal foot of pipe than the parallel arrangement. However, the series ground

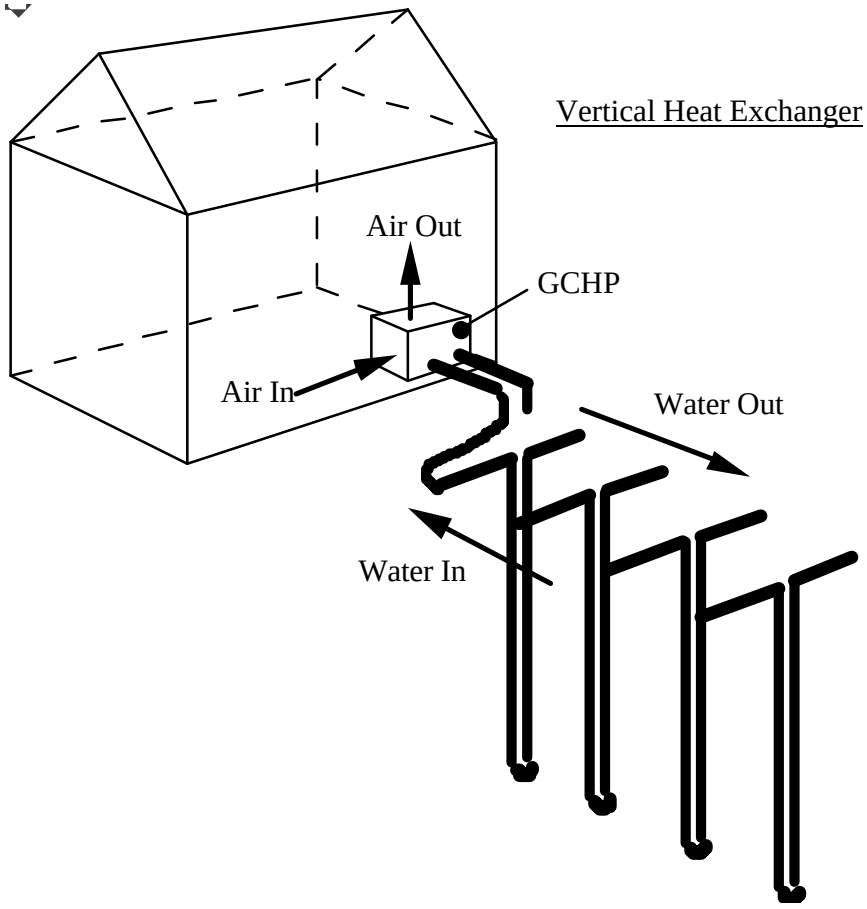

Figure 2.8 Vertical closed loop ground coupled heat pump

loops have significant disadvantages that cause them not to be favored by contractors. Large diameter pipe is heavy, expensive, needs a higher volume of anti-freeze solution, and the

layout requires long continuous trench lengths, all contributing to high installation costs. A parallel arrangement uses smaller diameter pipes so each branch of the fluid circuit maintains turbulent conditions at the lower flow rates. Parallel systems use less expensive, smaller diameter pipe, less anti-freeze solution, and require less continuous trench length. Due to their lower installation costs and convenient layout flexibility, parallel arrangements are almost always preferred to series.

CHAPTER
THREE

Models of heat pumps, as well as the locations, house size, and systems to be compared must be chosen to investigate the economics of GCHP in Wisconsin. The following sections contain a discussion of the choices that had to be made to develop a model adequate for the scope of this study. This chapter also describes in detail the models which were used in the simulations.

3.1 Equipment for Comparison

Heating and cooling systems had to be chosen for the economic comparisons of this report. The systems chosen had to be alternatives to the residential GCHP system. Resistance heating with vapor-compression air conditioning, gas furnace heating with vapor-compression air conditioning, and an air-source heat pump were chosen to be the systems against which the GCHP would be compared.

The desuperheater attachment is an important part of the energy savings that a GCHP can deliver. Traditional hot water tanks use electricity or natural gas to heat the water. The energy requirements of the traditional systems will be compared to an electrically heated tank augmented with a desuperheater.

3.2 TRNSYS or Bin Model

The two modeling approaches considered for this analysis were hourly simulations and the bin temperature method. A choice needed to be made as to which method would best generate the output needed for this analysis.

A transient analysis marches through time at a simulation time step and records output at a desired output time step. Depending on the models, the simulation time step could range from minutes to hours. The output time step can be set for whatever level of detail is necessary. An appropriate program for energy system simulations is TRNSYS (Klein, 1994), a transient system simulation software package in which components, called types, are modeled in FORTRAN code and linked together to form a system. A TRNSYS deck describes how the different types will interact with one another. A simulation time step is chosen that is suitable for the analysis, and information can be output as the program marches through each simulation time step of the year. An important aspect of this type of simulation is that the time of year or day that something occurs can be tracked, allowing a detailed analysis of the output. TRNSYS has the ability to read real weather data from any number of cities around the world and use it to drive a model. TRNSYS has available house, tank, and air conditioning equipment models, so that only controllers and a ground heat transfer model would need to be developed.

A bin temperature analysis breaks the air temperatures in a location into 5° bins on a monthly or yearly basis. For each temperature bin, the number of hours that the air temperature is within that particular bin range is tabulated. For example, if there are 100 hours during the year where the temperature falls between 74.5°F and 79.5°F, then there are 100 hours in the 77°F bin. The load on the house for each temperature bin is then calculated, and when

combined with the system COP and bin hours, a heating and cooling system energy consumption can be found.

With the bin analysis, there is no time dependency, so the order with which these loads occur is not known. There is no way to track the transient behavior of a system with capacitance, or to monitor at what time of day energy was used. This means that the desuperheater contribution to the hot water load, which depends on the coincidence of the need for water heating and heat pump operation, can only be roughly estimated. Since thermal capacitance cannot be modeled in a bin analysis, an approximation of the water temperature entering the heat pump has been developed (OSU, 1988). For this approximation, the water temperature is linked to the air temperature, following the logic that very cold winter days will have very low entering water temperatures and hot summer days will have very high entering water temperatures.

This bin method, shown as a line in Figure 3.1, associates the coldest desired water temperature with the coldest outdoor air temperature, and the hottest desired water temperature with the hottest outdoor air temperature. For example, if the air temperature is TA_{min}, the water temperature is EWT_{min}. However, the nature of the ground heat exchanger is that it is coupled to the ground temperatures of the area, and the temperature returning to the heat pump depends on time of year and previous operating loads. In reality, the entering water temperature is only a weak function of the ambient temperature, as shown in Figure 3.1 as a scatter plot. The scatter plot of EWT vs the ambient temperature was generated using the simulations from this project. Each dot on the graph represents a 2.5 minute period over which the GCHP was operating. During that 2.5 minute period, the average ambient air temperature and EWT were recorded for the plot.

If there were a series of cold weeks at TA_{min} which caused the EWT to drop to 25°F, a rapid increase of ambient temperature to TA_{mean} would not cause the EWT to increase rapidly to

EWT_{mean}. In this situation, the heat pump would continue to have an EWT near 25°F, reflecting the effects of the cold snap from the previous few weeks. The bin approximation would have the EWT experience the same rapid shifts in temperature that the air experiences. The system energy consumption predicted by this method is highly optimistic, due to the delivery of EWT which are less extreme than a real system would experience.

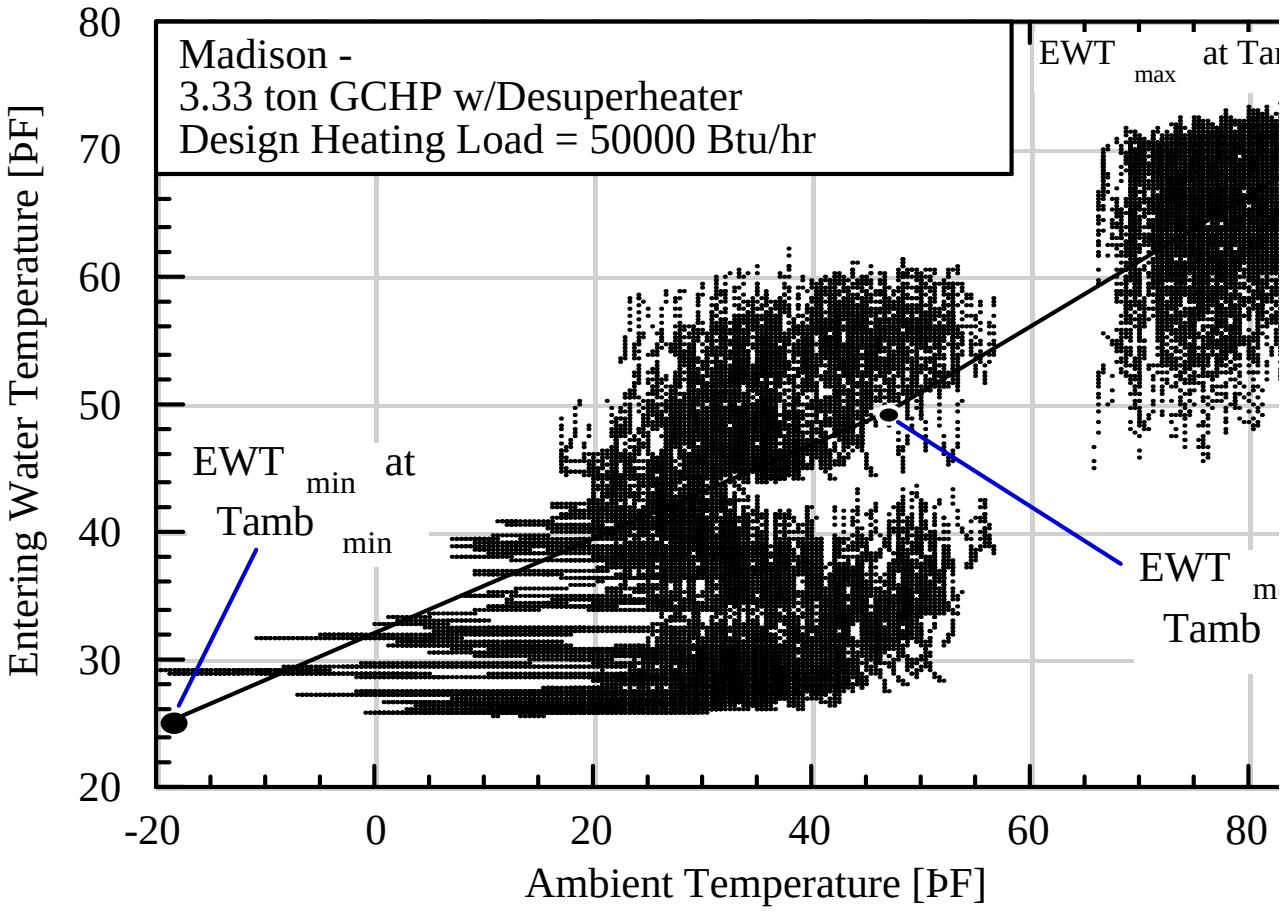

Figure 3.1 EWT vs. Ambient Temperature for a year simulation.

TRNSYS can be used to meet all of the analysis requirements. Since TRNSYS can track loads in time, on and off peak energy usage can be monitored. TRNSYS can also read in realistic hot water load profiles allowing desuperheater performance to be approximated. A ground heat transfer model could be written in FORTRAN and added to TRNSYS so that the water temperature entering the heat pump depends on the time of year, previous hours of

operation, and ground-loop length. For this project, TRNSYS was chosen to be the analysis tool.

3.3 Locations to be Examined

Typical Meteorological Year (TMY) weather data was used for the TRNSYS simulations. These data represent typical weather from a thirty year period and are available for many locations throughout the country at one hour intervals. In choosing locations for this analysis, availability of weather data was the limiting factor. Only five locations, Madison, Milwaukee, La Crosse, Green Bay, and Eau Claire were available in Wisconsin. Of the locations available, Madison and Eau Claire were chosen to represent two typical weather regions.

3.4 House Model

Utilities consider a typical Wisconsin house to have a 50,000 Btu/hr design heating load and a 30,000 Btu/hr design cooling load (WCDSR #1, 1994). These loads correspond to a ranch style home with 1500 ft^2 of floor space and moderate insulation. For this study, the thermostat will be set to 75°F for cooling and 68°F for heating with no thermostat set back.

TRNSYS type 12 was used to model the building loads. This type calculates the load using an overall heat transfer coefficient and the difference between the indoor and outdoor air temperatures. Thermal capacitance is modeled as a single lumped capacitance so the house temperature changes as it loses or gains energy. The house exchanges energy with the ambient air and experiences energy gains from internal and solar sources. The internal and solar energy gains make up what are called time variant gains. Internal loads are considered constant throughout the simulation. The solar gains are a function of time and are calculated using solar radiation records in the weather data in conjunction with an absorbtion coefficient. Equation 3.1 shows the energy balance equation for the type 12 structure.

$$C_{house}\frac{dT_R}{dt} = \dot{Q}_{gain} - UA*(T_R - T_{amb}) + \dot{Q}_{heat} + \dot{Q}_{sensible} \qquad (3.1)$$

It is assumed that the house maintains a constant relative humidity of 51.4% throughout the cooling season. This assumption had to be made since heat pump and air conditioner performance catalogs give data for only a few relative humidities. A relative humidity of 51.4% corresponds to 80°F dry bulb/67°F wet bulb or 75°F dry bulb/63°F wet bulb, and is a reasonable relative humidity for a comfortable room. Figure 3.2 shows a picture of the house and the various influences on the heat transfer.

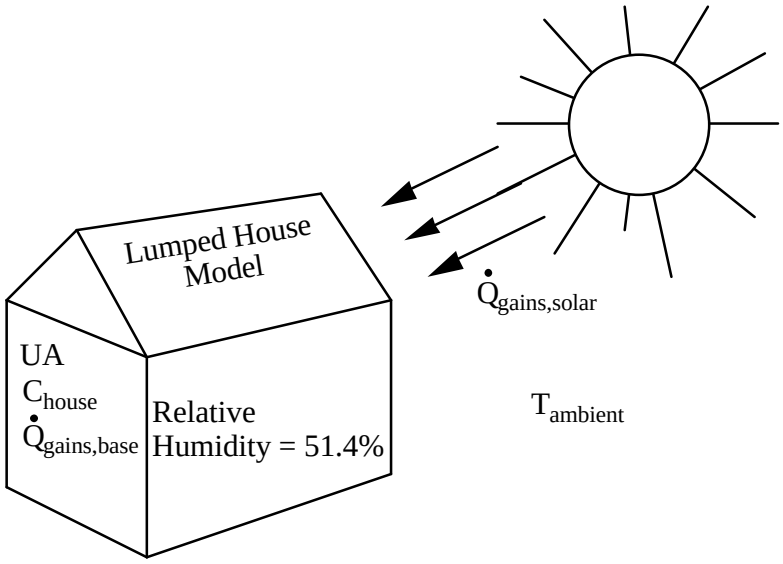

Figure 3.2 TRNSYS house model

To run this model the user needs to specify an overall heat transfer coefficient, an effective capacitance, an outdoor air temperature, and a time variant gain. Before these parameters can be found, a winter balance temperature must be assumed. The winter balance temperature is the outdoor temperature at which the internal gains exactly offset the house energy losses to the surroundings. If the ambient temperature falls below the balance temperature, the temperature of the house will decrease. If a house were to have no internal gains, the balance temperature would be the thermostat set point. A typical value for a house balance temperature would be around 60°F. This means that there are internal energy gains in the

house that can keep the house temperature from falling when the outdoor temperature is 60°F or above. The summer balance temperature, although not needed when solving for the house parameters, is 67°F.

The following equations were used to find the parameters which describe the house heat transfer characteristics.

$$\dot{Q}_{design,winter} = UA * (T_{set,winter} - T_{design,winter}) - \dot{Q}_{gains,base} \quad (3.2)$$

$$\dot{Q}_{gains,base} = UA * (T_{set,winter} - T_{balance,winter}) \quad (3.3)$$

$$\dot{Q}_{design,summer} = UA * (T_{set,summer} - T_{design,summer}) - \dot{Q}_{gains,max} \quad (3.4)$$

$$\dot{Q}_{gains,max} = \dot{Q}_{rad,max} + \dot{Q}_{gains,base} \quad (3.5)$$

$$\dot{Q}_{rad,max} = UA * \dot{I}_{horizontal,max} * \alpha/h_o * PerHsSun \quad (3.6)$$

ASHRAE design temperatures are used to find the house parameters (ASHRAE, 1993). For Madison, the winter design temperature that only 2.5% of days exceed is -7°F. The summer design temperature which only 2.5% of days exceed is 88°F. Given the heating load of 50000 Btu/hr, the ASHRAE winter design temperature, the winter balance temperature, and the winter thermostat set point, equations 3.2 and 3.3 are used simultaneously to give the UA and the base internal energy gains, $\dot{Q}_{gains,base}$. Next, having the summer cooling design load, UA, the summer thermostat set point, and the ASHRAE summer design temperature, equation 3.4 can be used to find the maximum energy gains, $\dot{Q}_{gains,max}$. Now, equation 3.5 can be used to find the value of $\dot{Q}_{rad,max}$. Finally, knowing the values of $\dot{Q}_{rad,max}$, UA, the maximum global radiation, and α/h_o, the fraction PerHsSun can be found using equation 3.6. The parameter values used in this report are listed in the Table 3.1.

Table 3.1 House parameters used in this report

		Madison	Eau Claire
Design Heating Load	Btu/hr	50000	53000
Design Cooling Load	Btu/hr	30000	28300
UA	Btu/hr-°F	0.746	0.746

ASHRAE Winter Design Temperature	°F	-7.0	-11.0
ASHRAE Summer Design Temperature	°F	88.0	89.0
Winter Set Point	°F	68.0	68.0
Summer Set Point	°F	75.0	75.0
Maximum Global Radiation	Btu/hr/ft^2	345.0	345.0
$Q_{gains,base}$	Btu/hr	5970.0	5970.0
α / h_o	ft^2 F hr/Btu	0.3	0.3
PerHsSn	dimensionless	0.184	0.184

3.5 Heating and Cooling Equipment Models

There are many different heating and cooling system types compared in this analysis. There are GCHP with and without desuperheaters, ASHP, baseboard resistance heating with an electric air conditioner, and gas furnace heating with an electric air conditioner. This section contains descriptions of the models used for each of the systems.

3.5.1 Resistance Heating

The model for resistance heating is the simplest of all of the models. Modeled as resistance heating without a circulating fan, the heater consists of a single stage element large enough to satisfy the greatest heating loads. The heating capacity is shown in equation 3.7.

$$HC = kW_{ht} * 3.413\left[\frac{Btu/hr}{kW}\right] \qquad (3.7)$$

It is assumed that all of the electrical energy going into the heating elements makes its way into the heated space, so the COP is 1.0. The operation of the resistance heater is regulated by a special TRNSYS type which operates as a deadband temperature level controller.

3.5.2 Natural Gas Furnace

The natural gas furnace has a single capacity which exceeds the greatest heating loads. This model includes an overall efficiency of 95%, which approximates a combustion efficiency and stack losses. Equation 3.8 shows the calculation to find the rate at which natural gas is used.

$$HC = \text{specified furnace heating capacity in } {}^{Btu}/_{hr}.$$

$$\frac{therm_{gas}}{hr} = \frac{HC}{\eta_{furnace} * 100000\left[{}^{Btu}/_{therm}\right]} \tag{3.8}$$

Included in the energy requirements for this system are parasitics associated with a circulating fan. For a reasonable circulating air flow rate of 1300 cfm, fan power is about 820 watts (Temperature Systems, 1994). The gas furnace and circulating fan are operated by a special controller, type 92, designed specifically for this system.

3.5.3 Vapor Compression Air Conditioner

The vapor compression air conditioner, used in the resistance and natural gas heated houses, was modeled using catalog performance data (Bryant,1991). The indoor circulating fan power, outdoor blower power, and compressor power are included in the total system power reported in the tables. Total cooling capacity and sensible cooling capacity are the other reported data. For intervals of 10°F, performance data are given for an indoor dry bulb temperature of 80°F at three circulating fan air flow rates with four indoor wet bulb temperatures. The wet bulb temperatures given are 72, 67, 62, and 57°F.

A real vapor-compression cycle has performance which is a function of two independent variables, the indoor *and* the outdoor air temperature. When TRNSYS type 42 (conditioning equipment) is used to model the air conditioner, a logical unit is created which contains a single independent variable and a number of dependent variables. For the air conditioner, the ambient temperature is the independent variable and total cooling capacity, system power, and sensible heat ratio are the dependent variables. Performance data are entered into the

logical unit for an indoor dry bulb temperature of 80°F, and a wet bulb temperature of 67°F, which gives a relative humidity of 51.4%. Type 42 reads in the logical unit and, given a value of the independent variable, interpolates the data to find the performance of the system. Since data is given only for an indoor temperature of 80°F, the performance values need to be adjusted if the indoor air temperature is other than 80°F. Any deviation from that dry bulb temperature is accounted for using performance correction factors (CF) given in the catalogs. Equation 3.9 calculates the correction factor used to adjust the value of the sensible capacity of the air conditioner. Equation 3.10 shows how this correction factor is used in the adjustment.

$$CF = 835 * \left(\frac{CFM}{1000 \left[\frac{ft^3}{min} \right]} \right) * \left(\overline{T}_R - 80ÞF \right) \left[\frac{Btu}{hr\ ÞF} \right] \tag{3.9}$$

$$\dot{Q}_{sens,corrected} = \dot{Q}_{sens,80ÞF} + CF \tag{3.10}$$

This is the only correction factor used in this project which is added to the 80°F performance data. The other correction factors, used with the ASHP and GCHP, are dimensionless values that are multiplied by the 80°F performance data during cooling, or the 70°F performance data during heating. Correction factors for the total power consumption were not given with the air conditioner catalogs. Adjustments to the power consumption were made using correction factors from the ground coupled heat pump performance data. Since the vapor compression cycles are similar, the correction factors should be similar. The correction factor is shown in equation 3.11, with the adjusted power shown in equation 3.12. Notice that this correction factor is a multiplier.

$$CF_{kW} = .68 + .004 * \overline{T}_R \tag{3.11}$$

$$kW_{cool,corrected} = kW_{cool,80ÞF} * CF_{kW} \tag{3.12}$$

3.5.4 Air-Source Heat Pumps

The air source heat pump (ASHP) was modeled using catalog performance data (Lennox, 1993). However, ASHP performance data are incomplete. Indoor and outdoor fan power are not included in the system power listed in the performance data tables. The catalog lists the outdoor blower power for each unit in the front of the catalog, but the indoor fan power must be approximated from circulating fan performance literature. Both indoor and outdoor fan power must then be added to the compressor power found in the data tables. Cooling data are supplied for typical ambient operating conditions in 10°F intervals. The cooling data are given for a number of dry and wet bulb combinations. For each combination of dry and wet bulb temperatures, the data contain total cooling capacity, sensible heat ratio, and compressor power for three indoor circulating air flow rates. Heating data for a large number of outdoor air temperatures are presented for one air flow rate and an indoor air temperature of 70°F. At low ambient temperatures, the heating capacity, COP, and compressor power are adjusted to include the effects of the defrost cycle.

Again, TRNSYS type 42 is used to model this system performance. Two separate type 42 units are needed, one for cooling and one for heating. Cooling is modeled in the same manner as the air conditioner in section 3.4.3. Heating is also modeled in a similar manner, except the heating logical unit contains heating capacity and operating power for different outdoor air temperatures. Since heating and cooling data are entered into logical units for only one indoor air temperature, correction factors are again used to adjust the performance data for different indoor temperatures. The ASHP catalog contains no correction factors, so correction factors were again used from the ground coupled heat pump catalog or calculated from data listed in the ASHP performance charts. The equations used to find the correction factors are listed below. In each of the following equations, CF is dimensionless value which is multiplied by the 80°F performance data when the internal air temperature deviates from 80°F.

The correction factor for the heating capacity was taken from the ground coupled heat pump catalog.

$$CF_{HC} = 1.21 - 0.003 * \overline{T}_R \quad (3.13)$$

The correction factor for total cooling capacity was derived using ASHP performance data.

$$CF_{TC} = 0.04 + 0.012 * \overline{T}_R \quad (3.14)$$

The following correction factors system power consumption were taken from the GCHP catalog.

$$CF_{kW,heat} = 0.65 + 0.005 * \overline{T}_R \quad (3.15)$$

$$CF_{kW,cool} = 0.68 + 0.004 * \overline{T}_R \quad (3.16)$$

The correction factor for the sensible heat ratio was derived using ASHP performance data.

$$CF_{SHR} = 1.64 - 0.008 * \overline{T}_R \quad (3.17)$$

Due to the drop in ASHP heating capacity during winter operation, auxiliary heat is required to meet the large winter heating loads. The effect of the auxiliary heat on the capacity and power of the system is shown in equations 3.18 and 3.19.

$$kW_{heat\ pump} = \left(kW_{compressor}\right) * CF_{kW} + kW_{fans} + kW_{resistance\ heat} \quad (3.18)$$

$$HC_{heat\ pump} = \left(HC_{80ÞF}\right) * CF_{HC} + 3413\left[\frac{Btu}{kW}\right] * kW_{resistance\ heat} \quad (3.19)$$

The auxiliary heat, which usually consists of resistance heating coils, is often broken into three stages which come on one at a time to meet the load. For this system, the auxiliary heat is regulated by a TRNSYS controller, which uses several deadband temperature levels to control the many stages of operation.

3.5.5 Ground Coupled Heat Pumps

The ground coupled heat pump was modeled using catalog performance data. Modeling the GCHP was more complicated than any of the other pieces of equipment due to the addition of a desuperheater and ground heat exchanger. Ground coupled heat pumps typically have two

stages of fan and/or compressor operation, with three stages of auxiliary resistance heat. The staged operation is controlled by a dead band thermostat which will be described in the following section.

Performance data as a function of water temperature entering the heat pump (EWT), were supplied for cooling at an indoor air temperature of 80°F dry bulb and 67°F wet bulb, for three circulating air flow rates and three heat exchanger fluid flow rates (WaterFurnace, 1992). Performance data for heating were supplied at 70°F, for three circulating air flow rates and three heat exchanger flow rates. Cooling data, supplied for EWT of 110, 90, 70, and 50°F, includes total cooling capacity, sensible cooling capacity, total system power, and heat rejected to the water by the condenser. Heating data, supplied for EWT of 90, 70, 50, and 30°F, include heating capacity, total system power, and heat extracted from the water by the evaporator. The total system power given in the performance tables include only indoor circulating fan and compressor power. Power requirements for the well and closed loop pump need to be calculated separately. Both heating and cooling data are supplied for systems with and without desuperheater operation. Since the EWT in a typical installation will fall below 30°F, the data was extrapolated down to 20°F.

Type 42 was also used to model the GCHP. Logical units, with EWT as the independent variable, were used for both heating and cooling operation. The cooling logical unit contained total cooling capacity, total system power, heat rejected to the surroundings, and sensible heat ratio for an indoor temperature of 80°F dry bulb, 67°F wet bulb. The heating LU contained heating capacity, total system power, and heat extracted from the water flow for an indoor temperature of 70°F

Correction factors were given by the ground-coupled heat pump manufacturer for different indoor air temperatures and converted to an equation form, in equations 3.20 - 3.26 (WaterFurnace, 1992).

$$CF_{HC} = 1.21 - 0.003 * \overline{T}_R \quad (3.20)$$

$$CF_{HE} = 1.42 - 0.006 * \overline{T}_R \quad (3.21)$$

$$CF_{TC} = -0.28 + 0.016 * \overline{T}_R \quad (3.22)$$

$$CF_{HR} = 0.04 + 0.012 * \overline{T}_R \quad (3.23)$$

$$CF_{kW,heat} = 0.65 + 0.005 * \overline{T}_R \quad (3.24)$$

$$CF_{kW,cool} = 0.68 + 0.004 * \overline{T}_R \quad (3.25)$$

$$CF_{SHR} = 1.64 - 0.008 * \overline{T}_R \quad (3.26)$$

To find the correct performance value when the indoor air temperature deviates from 80°F during cooling, or 70°F during heating, multiply the value returned from the logical unit by the correction factor.

Since the GCHP total system power only includes the indoor circulating fan and the compressor, the pump power required for the heat exchanger loop or well pump must be approximated. Closed loop pumping power was calculated as a function of Reynolds number and pipe length. The power of the pump was approximated assuming efficiencies of 77% and 85% for the pump and motor, respectively. The motor efficiency is typical of electric motors, and pump efficiency was approximated using some operating values given by the GCHP company. The following equations, 3.27 and 3.28, were used in the calculation of approximate pumping requirements.

$$\hat{W} = \frac{W_{fluid}}{m} = -\frac{1}{2}\langle\overline{v}\rangle^2 * \left[\frac{L}{R_h} f + e_v\right] + g h_{loss,HX} \quad (3.27)$$

$$Power_{pump} = \frac{\hat{W} * \dot{m}}{\eta_{motor} * \eta_{mech}} \quad (3.28)$$

Head losses through the heat exchanger, $h_{loss,HX}$, were given in the GCHP catalog for different loop flow rates.

Well-source pumping losses were backed out of the ARI 325 performance ratings given in the catalog (WaterFurnace, 1992). This rating includes the pumping power for each heat pump model assuming a typical well source system.

The ability of the GCHP to heat domestic hot water needed to be modeled. As discussed in chapter 2.3, the hottest part of the vapor compression cycle can be used to meet some of the hot water load. The refrigerant flows into the desuperheater at point B on Figure 2.1. During the cooling cycle, energy, that would have been sent to the ground heat exchanger as waste heat, is transferred into the water tank. Changing the destination of this waste heat has little effect on cycle operation. The heating cycle is more disturbed by the addition of the desuperheater. On Figure 2.1, the total heating capacity lies between the points B and D. Activating the desuperheater takes a portion of the heating capacity away from the house and directs it into the water tank.

The heating, cooling, and desuperheater capacity are functions of the EWT and the temperature of the tank water entering the desuperheater. A model had to be developed which accounted for changes in both of these temperatures, while also modeling the linked behavior of desuperheater capacity and the heating capacity.

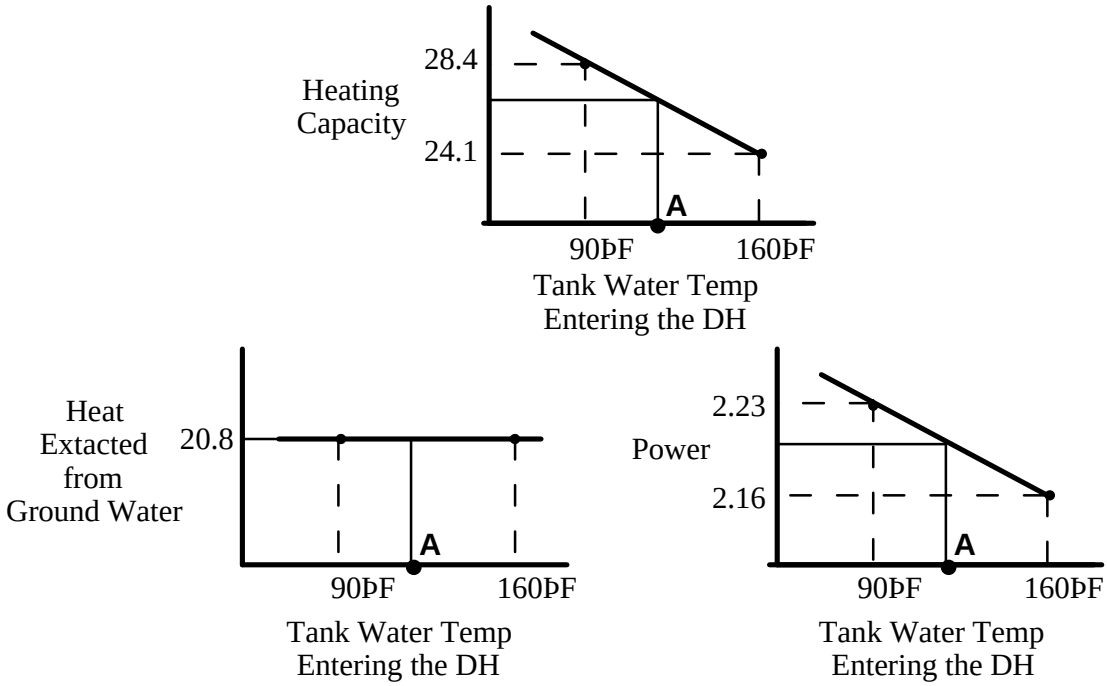

Figure 3.3 Linear interpolation of performance data to approximate GCHP performance as a function of desuperheater inlet temperature

A simple model was developed using the only two desuperheater performance points that were known. The catalog gives performance data for heat pump operation with no desuperheater. It also has performance data for a system with desuperheater operation where the water entering the desuperheater is 90°F at 0.4 gpm/nominal ton. From the manufacturer it was learned that the hottest refrigerant temperature was approximately 160°F (Meyer, 1994). If water from the tank were entering the desuperheater at 160°F there would be no heat transferred from the refrigerant to the water, mimicking the situation when there was no desuperheater operation at all. System operation when the tank water entering the desuperheater is not 90°F or 160°F was determined using an interpolation. For this interpolation, a 90°F tank water temperature coincides with the desuperheater performance data and a 160°F tank water temperature coincides with heating only performance data. Figure 3.3 shows this more clearly.

For each of the graphs in Figure 3.3, the performance values on the vertical axis are a function of the EWT and are updated for each TRNSYS time step. The 90°F points are for a heat pump operating with a desuperheater. The 160°F point are for a heat pump operating without a desuperheater. The operating values of heating capacity, heat extraction, and power are connected to their respective temperatures by dashed lines in the above Figure. For heating capacity, at the top of Figure 3.3, if the water entering the desuperheater from the hot water tank is at 90°F, the heating capacity will be 28.4 MBtu/hr. If the water temperature is 160°F, the heating capacity will be 24.1 MBtu/hr. When the tank water is in between these two temperatures, as with point A, a linear interpolation between 90°F and 160°F is performed. This interpolating procedure is the same for both heating and cooling. Since the tank water remains between 70°F and 125°F, this linear interpolation is hoped to be accurate enough for this project analysis.

3.6 Thermostat Model

The controllers for the heating and cooling equipment were designed for each system operation. While all the controllers operate as deadband thermostats, some also control air flow rates, pumping operation, loop flow rates, auxiliary heat, and desuperheater operation. The logic which is employed in all of the thermostats is discussed in this section.

For the thermostat controller, each level of operation is assigned a status. A higher status means a higher level of heating or cooling capacity. The status level is changed when a given temperature level is crossed. Temperature levels are arranged as shown in Figure 3.4. The logical sequence of the thermostat is shown in Figure 3.5. At the beginning of each TRNSYS

Temperature Levels

TU3 = Tset + 1.5ÞF	Stage 1 OFF
TU2 = Tset + 1.0ÞF	Stage 2 OFF
TU1 = Tset + 0.5ÞF	Auxiliary OFF
Tset = 68.0ÞF	Thermostat Set-Point
TL1 = Tset - 0.5ÞF	Stage 1 ON
TL2 = Tset - 1.0ÞF	Stage 2 ON
TL3 = Tset - 1.5ÞF	Auxiliary ON

Figure 3.4 Thermostat temperature levels

time step, the house temperature is checked. The controller is then called, and knowing its current status, and knowing the current room temperature, the status can either be increased or decreased. For instance, following Figure 3.5, if the current status is 3 and after the last TRNSYS time step the room temperature was 68.6°F, using the temperature levels of Figure 3.4, the status would be downgraded from 3 to 2, turning off the auxiliary heat so the house is being heated by only the second stage of heat pump capacity.

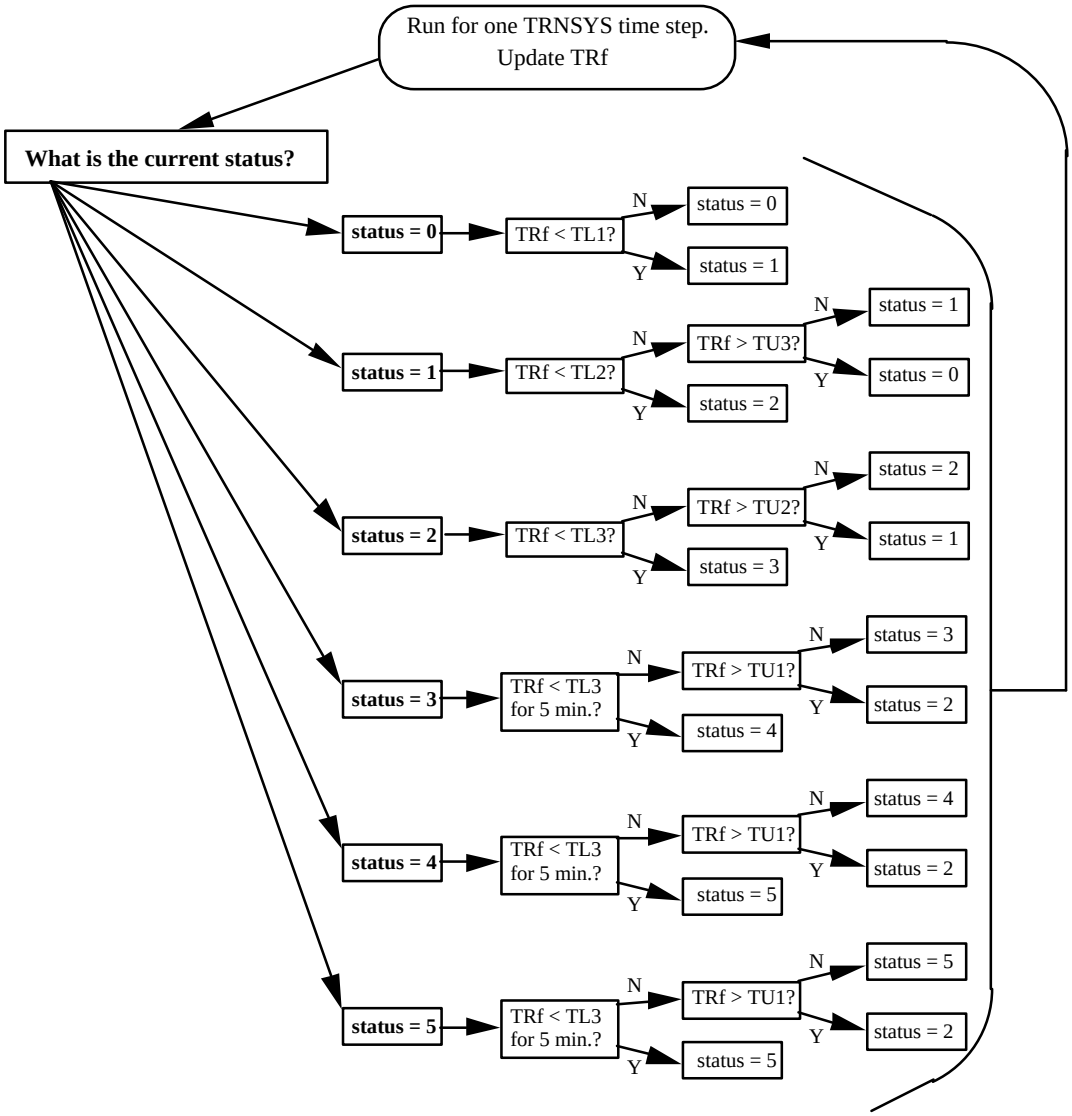

Figure 3.5 Logical sequence of thermostat

The thermostat logic when applied to the house model will allow for temperature variations similar to those shown in Figure 3.6 for a GCHP unit.

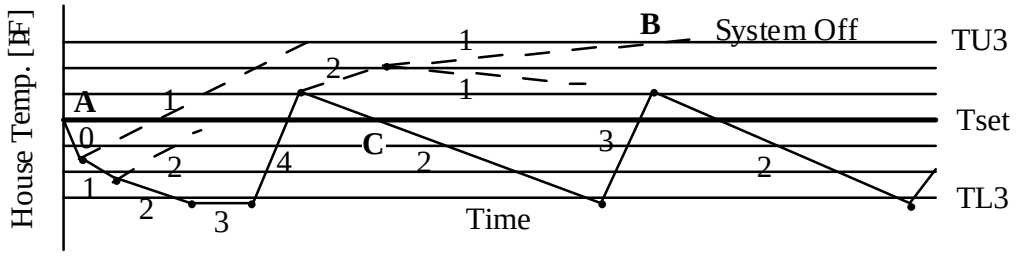

status 0 = System Off

status 1 = First Stage of Compressor

status 2 = Second Stage of Compressor

status 3 = 2 + 1st Stage of Auxiliary Heat

status 4 = 3 + 2nd Stage of Auxiliary Heat

status 5 = 4 + 3nd Stage of Auxiliary Heat

Figure 3.6 Thermostat Operation - Temperature Levels and Options

At point A of Figure 3.6, the system is turned off. As the temperature of the house decreases with time, the first temperature level is crossed. The status of the thermostat is increased from 0 to 1. When the status is increased the house temperature could react in different ways. The new capacity could exceed the house load and the temperature could increase (following the dashed temperature line), or the new capacity could be inadequate to meet the house load and the temperature could continue to drop (the solid temperature line). If the house temperature continues to drop, another temperature level will be crossed. This controller does not allow the system to return to a status of 0 unless it can be achieved by the status level 1, shown by point **B**. The line passing by point **C** shows a situation where status 2 is not enough to meet the load. In this situation, the controller will cycle the auxiliary on and off while keeping the heat pump in operation. Each system uses a slightly modified version of this controller.

3.7 Hot Water Tank Model

A desuperheater can be attached to a hot water tank in many ways. A conventional set-up shown in Figure 3.7 was used (WaterFurnace, 1990) for the simulations. In this system, the desuperheater draws from the bottom of an 80 gallon tank and returns the heated water back to the bottom of the tank. The water flows through the desuperheater at 0.4 gal/min/nominal ton. The thermostats are set to 120°F for the top element and 100°F for the bottom element.

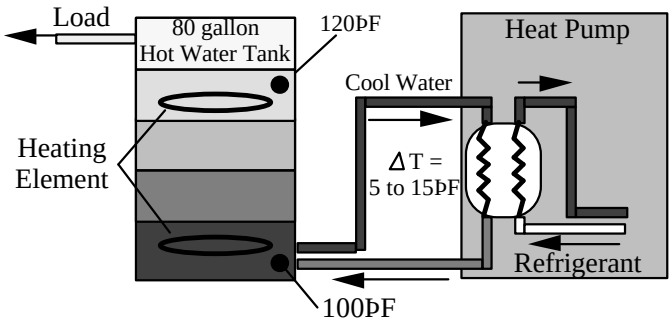

Figure 3.7 Desuperheater design for GCHP models

The heating capacity of the desuperheater is determined using the results of the interpolating procedure from section 3.4. During the heating season, the values returned from the interpolation are heating capacity (HC), heat extraction (HE), and power (KW_{heat}). Equation 3.27 is used to find the desuperheater capacity (HW).

$$HW = HE + KW_{heat} - HC \tag{3.27}$$

The water temperature leaving the desuperheater is calculated with equation 3.28.

$$T_{DH,out} = T_{DH,in} + \frac{HW}{\dot{m}_{DH}\, c_{p,water}} \tag{3.28}$$

The flowrate of the water through the heat exchanger should be set such that $T_{DH,out}$ is 5 to 15°F warmer than $T_{DH,in}$.

3.8 Modeling of the Entering Water Temperature

Ground coupled heat pumps in operation are supplied with a continuous flow of antifreeze or water. The performance of the heat pump depends on the temperature and flowrate of this fluid. For the TRNSYS ground coupled heat pump to operate it must be supplied an EWT for every simulation time step. The two GCHP water sources used in this report are horizontal closed loop and well source.

For well source heat pumps, water is taken from reservoirs that are 50 to over 100 feet beneath the surface. Temperatures at these depths are essentially constant throughout the year, at the mean annual ground surface temperature, T_{mean}. This value is given in IGSHPA installation manual (OSU, 1988) for a large number of geographic locations. In the TRNSYS model, the well source heat pump is supplied with a constant EWT of Tmean at the flow rate specified in the manual (WaterFurnace, 1992) for that heat pump model.

A GCHP with a closed loop heat exchanger has entering water temperatures that vary seasonally and depend strongly on the heat rejected to or extracted from the ground. A special TRNSYS type was created that can model the thermal capacitance and heat transfer of the soil around the buried pipe. This type is discussed in detail in chapter 4.

CHAPTER
FOUR

GROUND HEAT EXCHANGER MODEL

For this project, a ground heat exchanger model was needed that could deliver a return water temperature that depended on length, depth, hours of operation, time of year, and soil type. The model had to simulate a real system where the entering water temperature (EWT) changes as the system operates. The goal was to design a model that would approximate the entering water temperature without requiring significant computational time.

4.1 Finite Difference

Three methods that were available to model the EWT were investigated. These three methods were the line-source theory, bin temperature approximation, and finite difference modeling.

Line-source theory, often used in ground heat exchanger sizing, assumes that a pipe is buried in a large cylinder of soil. The temperature at the outer edge of the soil is that of undisturbed soil, called farfield conditions, and is determined using the temperature profile discussed in section 4.4. The farfield radius increases with time as the temperature around the pipe increases or decreases. The solution assumes a steady state temperature profile in the soil with a constant energy flux along the entire pipe length and no temperature gradients in the axial direction. Use of the model requires that the temperature leaving the pipe and the energy load on the pipe are specified. If the farfield radius and temperatures are known, the line source theory will return the length of pipe needed to absorb the desired energy with the

desired outlet temperature. The line-source theory was not chosen because the temperature profile in the soil is a steady state profile at all times. This means that it does not model the thermal capacitance of the soil, an important effect in a transient simulation.

Another approach would be to use the approximation designed for bin analysis. This method, where the entering water temperature is a function of the ambient air, was discussed in chapter 3.1. This was not a desirable method since the EWT is entirely decoupled from the ground. This simple approximation has no ground capacitance effects, where the previous operation determines the future EWT.

A third method, finite difference modeling of the ground, was chosen. Finite difference modeling allows the transient behavior of systems with thermal capacitance to be modeled. The material of interest is divided into a grid of nodes, each having a thermal capacitance determined by its volume and specific heat. Energy transfer between nodes uses Fourier's law of heat transfer, where the temperature difference between the nodes drives the energy transfer and the materials conductivity determines at what rate the energy is transferred. The temperature for each node is updated by stepping through time. Finite difference modeling is ideal for the needs of this project since the nodes can “remember” the effects of the previous hours of operation. Finite difference allows boundary conditions, such as farfield temperatures and inlet water temperature, to be changed arbitrarily.

4.2 Soil Properties and Behavior

Before building a model, it is necessary to understand the physical characteristics of soils and the phenomena that occur during ground heat transfer. Soil can have many different values of moisture level, specific heat, conductivity, and density, each of which is important in determining the final pipe length and performance of the system. Phenomena effecting energy transfer include heat transfer, soil moisture migration, and freezing.

For modeling purposes, the soils can be broken down into five different types. Table 4.1 lists the heat transfer characteristics of these soils (OSU, 1988). In reality, soil properties will vary seasonally, with location, and with depth. Soils in Wisconsin are generally moist and sandy with properties falling between those of heavy damp and light damp soils.

Table 4.1 Thermal Properties of Soils

	Thermal Conductivity [Btu/hr-ft-°F]	Thermal Diffusivity [ft^2/day]	Density [lbm/ft^3]	Specific Heat [Btu/lbm-°F]
Heavy Soil Saturated	1.40	0.84	200	0.20
Heavy Soil Damp	0.75	0.60	131	0.23
Heavy Soil Dry	0.50	0.48	125	0.20
Light Soil Damp	0.50	0.48	100	0.25
Light Soil Dry	0.20	0.26	90	0.20

Soil freezing is one seasonal variation that occurs near the ground surface and around the pipe. As soil freezes around the pipe it transfers latent energy to the fluid passing through the pipe. Frozen soil also has thermal properties that are more conducive to heat transfer than non-frozen soil. Both of these effects are beneficial to the performance of the ground heat exchanger, increasing the effectiveness during the worst winter months.

Soil moisture migration occurs during both the heating and air conditioning season, but is most significant during air conditioning. As the pipe rejects heat to the soil, there are temperature gradients near the pipe. Moisture will follow the gradients from hot to cold, drying the soil around the pipe. Dry soil has a lower thermal conductivity than moist or saturated soil, as shown in Table 4.1. If the soil thermal conductivity decreases, the effectiveness of the buried heat exchanger decreases causing the EWT to increase. Another problem caused by moisture migration is that the drying soil shrinks, creating air gaps around

the pipe. Air gaps increase contact resistance between the pipe and soil and can dramatically decrease the effectiveness of the buried heat exchanger. If significant drying occurs with a ground heat exchanger designed for moist soil conditions, serious problems could arise. The EWT could exceed the suggested upper limits recommended by the heat pump manufacturer.

4.3 Oak Ridge National Lab Model

A finite difference model was found that was capable of providing the EWT in a manner necessary for this project. Oak Ridge National Labs (ORNL) designed this model in the mid-1980's for use with ground-coupled heat pumps. Assumptions were made that simplified the heat transfer model. First, it was assumed that soil properties were uniform and constant throughout field, which meant no moisture migration or freezing occurs at any time. Secondly, it was assumed that the soil temperatures were not significantly disturbed by the buried pipe at a radial distance of four feet.

The assumptions used in the ORNL model are reasonable for the current project scope. Not including moisture migration, freezing, and changing soil characteristics greatly simplifies the FORTRAN code. However, these assumptions are justifiable for other reasons. Moisture migration and the resulting drying of soils is not a problem in areas with frequent rainfall and mild summers. Contractors in northern states report that they have not encountered problems with soil drying out around their heat exchangers. In the Residential Earth-Coupled Heat Pump Demonstration, it was reported that there were no adverse affects due to moisture migration during the cooling season (Hughes, 1985). For this project, since the cost of cooling only accounts for 10 to 15% of the energy demands of the GCHP, ignoring the effects of moisture migration will have little effect on the economic analyses performed on a GCHP system.

Freezing certainly could be considered an important effect in Wisconsin soils. Papers suggest that ignoring this effect will mean that the heat exchangers will be oversized. If pipes of the same length were used for a model with freezing and a model without freezing, the model with freezing would perform better due to higher EWT resulting from the increased ground heat exchanger effectiveness caused by the freezing. Therefore, for a real Wisconsin system to achieve the same performance predicted by this model, the actual heat exchanger should be shorter in length.

A paper by Mei and Emerson (Mei, 1985) refers to a study that showed that the soil near a buried pipe was not significantly disturbed beyond a radial distance of four feet. Therefore, using this assumption, farfield temperatures could be maintained at an outer radius of 4 feet from the pipe without significant errors.

4.4 Oak Ridge National Lab Model - Description

This section, 4.4, briefly describes the model developed at ORNL. A description of the TRNSYS model follows in section 4.6.

The ORNL model breaks the buried pipe length and a surrounding cylinder of soil into axial sections (Mei, 1986). Each section is then divided into a nodal network as in Figure 4.1.

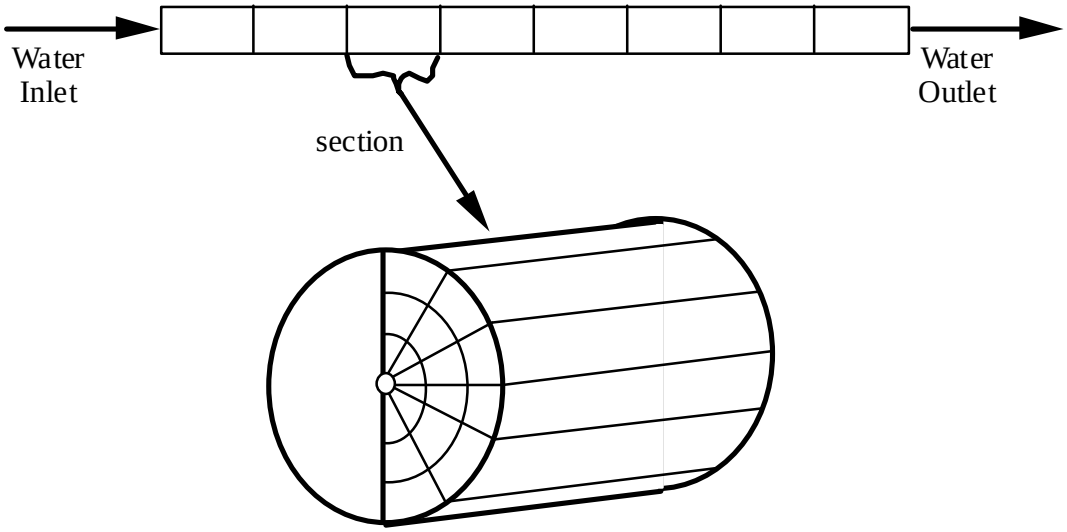

Figure 4.1 Length divided into axial sections

The pipe is located at the center of the cylinder of soil. Immediately surrounding the pipe is a cylinder of backfill. Backfill can be any number of heat transfer enhancing materials often poured or packed around a buried pipe. If no backfill is desired, properties of the surrounding soil could be used. Soil heat transfer by conduction occurs both radially and circumferentially. The energy transfer in the soil, pipe wall, and backfill is described by partial differential equations. The partial differential equation for heat transfer in the soil is shown in equation 4.1. Solutions are found for the partial differential equations by converting them into finite difference equations.

$$\frac{\partial^2 T_{soil}}{\partial r^2} + \frac{1}{r}\frac{\partial T_{soil}}{\partial r} + \frac{1}{r^2}\frac{\partial^2 T_{soil}}{\partial \theta^2} = \frac{1}{\alpha_{soil}}\frac{\partial T_{soil}}{\partial t} \qquad (4.1)$$

Mass and energy balances are performed on the fluid in each axial section, where the fluid is treated as fully mixed throughout each section. Equation 4.2 is the partial differential equation which describes the energy balance on each fluid node.

$$\frac{\partial T_f}{\partial t} = -V\frac{\partial T_f}{\partial x} + \frac{2}{r_o r_f C_f} q'' \qquad (4.2)$$

The fluid exchanges energy with the inside pipe wall based on the following relation, equation 4.3.

$$q'' = h\left(T_p - T_f\right)_{r_o} = K_p \left.\frac{\partial T_p}{\partial r}\right|_{r_o} \tag{4.3}$$

The effect of the convection coefficient, h, in equation 4.3 was investigated in the ORNL report to determine whether or not convection within the pipe was a significant contributor to the resistance of energy flow. Answering this question would reveal the accuracy required for the calculation of the convection coefficient. It was found that the thermal resistance due to convection was only a factor when the flow became laminar. As long as the flow was turbulent, the heat transfer from the pipe to the soil did not change significantly as the heat transfer coefficient was changed. Since the value of the convection coefficient did not effect the solution as long as flow was turbulent, the ORNL model assumed a value of Nusselt number that was representative of the type of turbulent flow found in a ground heat exchanger. Flow in ground heat exchangers is turbulent, near the transition from laminar to turbulent.

A finite difference model has a time step below which the numerical solution will become unstable. This is called a critical time step, and is the thermal capacity of the node divided by the sum of the surrounding thermal resistances. This is calculated using equation 4.4.

$$dt_{i,critical} = \frac{mass_i * c_{p,i}}{\sum \frac{1}{R_{ij}}} \tag{4.4}$$

For the ORNL model, the smallest critical time step was approximately 0.05 minutes, and occurred in the nodes representing the pipe wall. However, the smallest soil node had a critical time step of around one minute. If the entire node updating procedure were performed at the time step of 0.05 minutes, it would take days to complete a one hour simulation. In order to shorten the simulation time, two time step levels were used. The first

time step level of 0.05 minutes was used to update the fluid and pipe temperatures. The second time step level of 0.75 minutes was used for the backfill and soil nodes.

The farfield temperatures, or the temperatures at the outer boundary of the cylinder of soil are a function of time and depth. ORNL used a function derived by Kusuda which estimates the seasonal variation of ground temperatures with depth (Kusuda, 1965). This approximation is given in equation 4.5.

$$T(Z_{depth}, t_{year}) = T_{mean} - T_{amp} * \exp\left\{-Z_{depth}\left(\frac{p}{365 * a_{soil}}\right)^{1/2}\right\} * \cos\left\{\frac{2p}{365}\left[t_{year} - t_{shift} - \frac{Z_{depth}}{2}\left(\frac{365}{p\, a_{soil}}\right)^{1/2}\right]\right\} \quad (4.5)$$

T_{mean} is the mean value of the ground surface temperature for a specific location over an entire year. T_{amp} is the amplitude that the surface temperature experiences throughout a year at that location. The surface temperatures lowest value will be T_{mean} - T_{amp}, and its highest value will be T_{mean} + T_{amp}. The parameter t_{shift} is the difference in time between the beginning of the calendar year and the occurrence of the minimum surface temperature. Values of T_{mean}, T_{amp}, and t_{shift} are given for different geographic locations. The range of temperatures generated by this equation is shown in Figure 4.2. Line W shows one extreme that the temperature profile assumes during the winter season. Line Su shows the other extreme that the temperature profile assumes during the summer. In between summer and winter extremes, ground temperatures will fall between lines W and S.

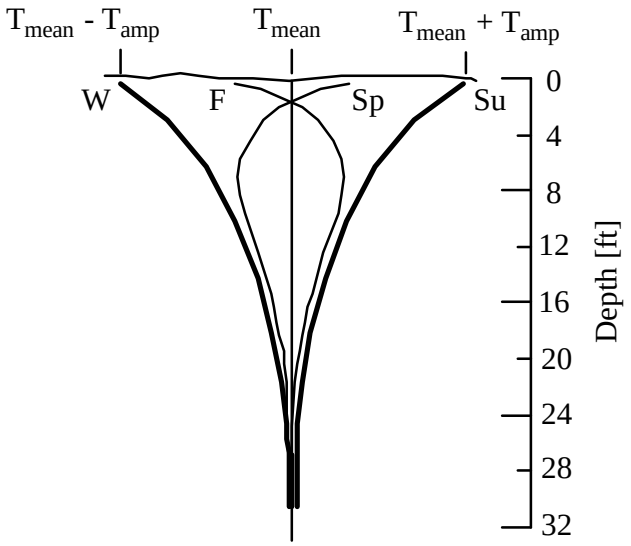

Figure 4.2 Kusuda ground temperature profiles with depth

In the spring, as the surface temperature increases, the deeper ground temperatures rise more slowly, as shown with line Sp. In the fall, as the surface temperature decreases, the deeper temperatures cool down more slowly, as shown by line F.

4.5 Improvements on the ORNL Model

Upon close examination of the ORNL FORTRAN code, areas were found where improvements had to be made. Some of the improvements were made to customize the program for the particular needs of this project. Other changes were made due to errors discovered in the ORNL code.

The first problem with the ORNL model was its slow computational speed. The reason for this slow speed was the high level of detail with which the model was built. Small nodes were created in the pipe and backfill regions to track their temperature with respect to time. A very small mass will cause the numerator in equation 4.4 to become very small, creating a tiny critical time step; discussed in the last section, the smallest critical time step was less

than 0.05 minutes. Figure 4.3 shows the nodal network around the pipe for the ORNL model. The pipe and backfill region are divided into two nodes each.

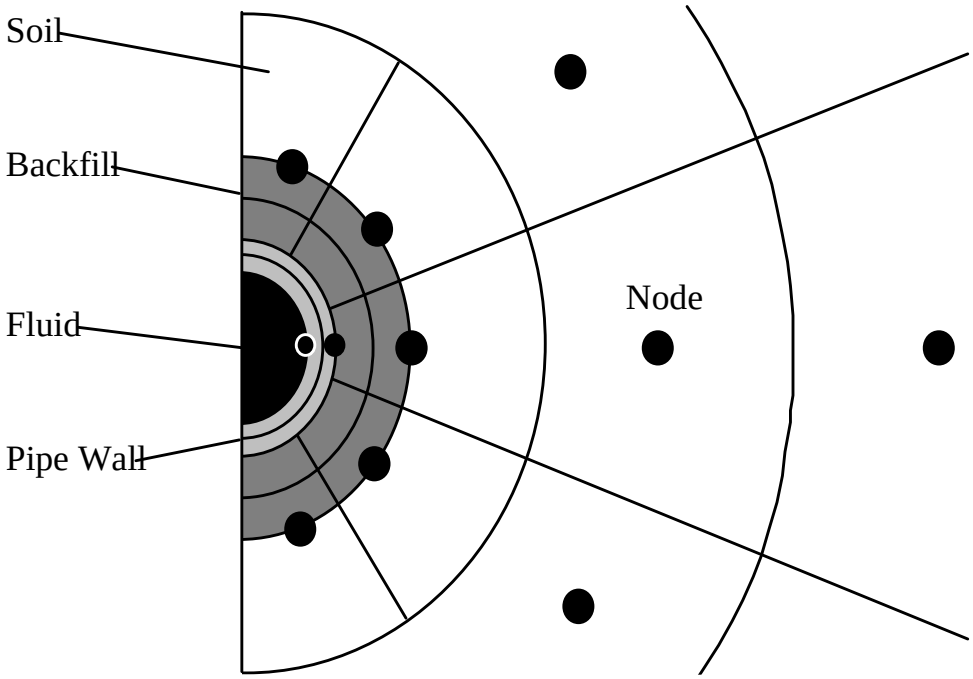

Figure 4.3 ORNL model for heat transfer around pipe

Tracking these temperatures at such small time steps is unnecessary when the critical time step of the soil around the pipe is 20 times larger. Their contribution to the resistance of heat transfer, however, is important. A model which includes the pipe and backfill resistance and mass contributions while eliminating the tiny critical time step will be discussed in the next section.

Another problem with the ORNL model was that a fluid element, or a temperature front, does not pass through the length of the pipe in the correct amount of time. For instance, if a flow rate of 100 ft/min were used with a 1000 ft pipe, it should take 10 minutes for any temperature changes at the inlet to pass through the pipe. The ORNL model passed the inlet variations immediately through the pipe. This problem was traced to an incorrect updating procedure for the fluid temperatures in the FORTRAN code. The original code updates each

section, from the fluid to the outermost nodes, for each time step before moving to the next section. When the first section is initially updated, the update begins with every temperature at time zero and ends with every temperature updated to the new time level. Section two should also begin with every temperature at time zero, because the fluid flowing into section two is the fluid leaving the first section at time zero. This was not the case with the ORNL code. Section two mistakenly had water flowing into it which was at the updated time level. This caused a temperature front to move through the entire length of tubing almost instantly. Changes needed to be made to correct this error and decrease the computational time of the ground model. It was decided that to implement these changes the entire ORNL model would be gutted and used only as a skeleton for the improved version.

4.6 Description of the TRNSYS Ground Heat Exchanger Model

As discussed, the new model uses the ORNL model as a base. The soil grid structure and farfield temperature calculation were not changed. This section contains a detailed description of the TRNSYS ground heat exchanger model.

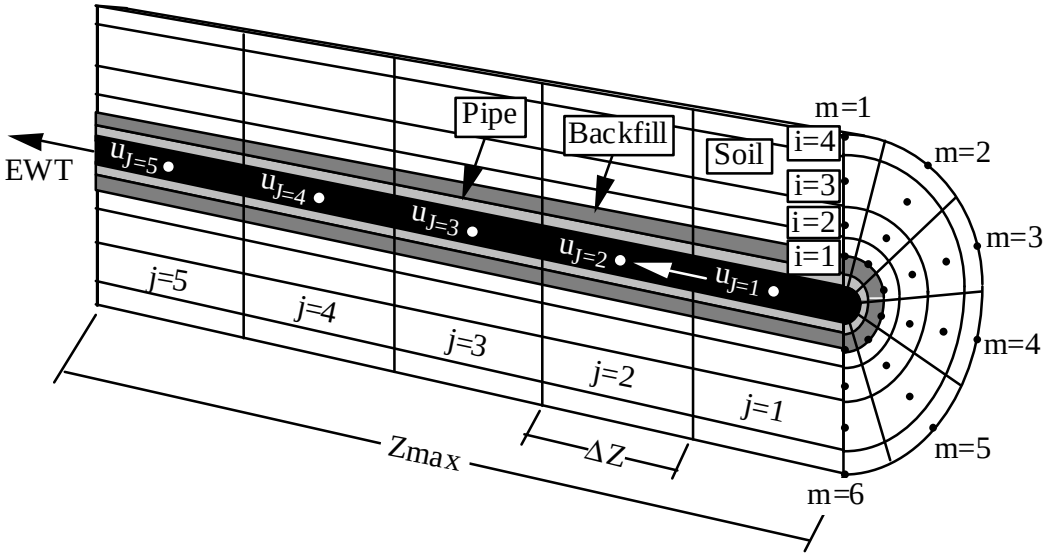

Figure 4.4 Labeling of nodes for finite difference grid.

The new model has the pipe located at the center of a large cylinder of soil. The cylinder of soil is then divided into axial sections along the buried pipes length. The heat transfer is symmetric about a vertical line passing through the center of the pipe, so only half of the cylinder needs to be modeled. Heat flow can travel radially and circumferentially, but not in the axial direction. This is a good assumption since in the axial direction distances are large and temperature differences are small. Farfield boundary temperatures are given by equation 4.5, the Kusuda relation. The ORNL soil property assumptions are used for this model. Figure 4.4 shows a sample grid layout. Nodes are labeled for section (j), radius (i), and rotation from the top (m). The variable k marks whether or not a node has been updated. Fluid temperatures are tracked with the variable array U(j,k). The rest of the soil temperatures are tracked in the array S(i,j,m,k).

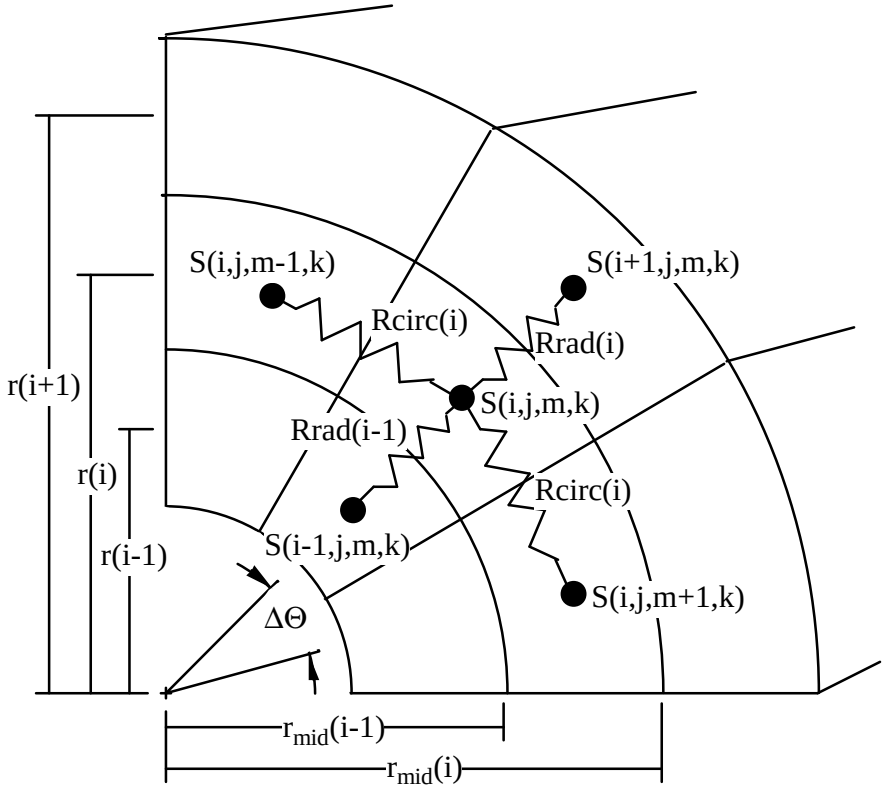

Figure 4.5 Resistances from a soil node to surrounding soil nodes

The radial and circumferential heat transfer were modeled using the thermal resistance approach. Although the thermal resistance approach to heat transfer is based on the same partial differential equations used in the ORNL model, the thermal resistance approach is superior due to its simplicity in concept and implementation. Figure 4.5 shows how the resistances were arranged.

The values of the resistances in Figure 4.5 are defined as follows in equations 4.6 and 4.7.

$$R_{circ}(i) = \frac{r(i) * \Delta\theta}{k_{soil} * \left(r_{mid}(j) - r_{mid}(j-1)\right) * \Delta Z} \tag{4.6}$$

$$R_{rad}(i) = \frac{\ln\left(r(i+1)/r(i)\right)}{\Delta\theta * k_{soil} * \Delta Z} \tag{4.7}$$

Using these values of R_{circ} and R_{rad}, the temperature of soil node, S(i,j,m,k), is updated using equation 4.8.

$$(\rho V(i)c)_{soil}\frac{(S(i,j,m,k+1)-S(i,j,m,k))}{dt}=\frac{(S(i+1,j,m,k)-S(i,j,m,k))}{R_{rad}(i)}$$
$$+\frac{(S(i-1,j,m,k))}{R_{rad}(i-1)}+\frac{(S(i,j,m+1,k)-S(i,j,m,k))}{R_{circ}(i)}+\frac{(S(i,j,m-1,k)-S(i,j,m,k))}{R_{circ}(i)}$$

(4.8)

The critical time step of the new model was increased by simplifying the ORNL grid structure. The node structure shown previously in Figure 4.3 led to very small critical time steps. In the new approach, shown in Figure 4.6, a slice of the pipe mass, a slice of the backfill mass, and a small section of soil are included in the mass of the innermost nodes. Energy transferring from

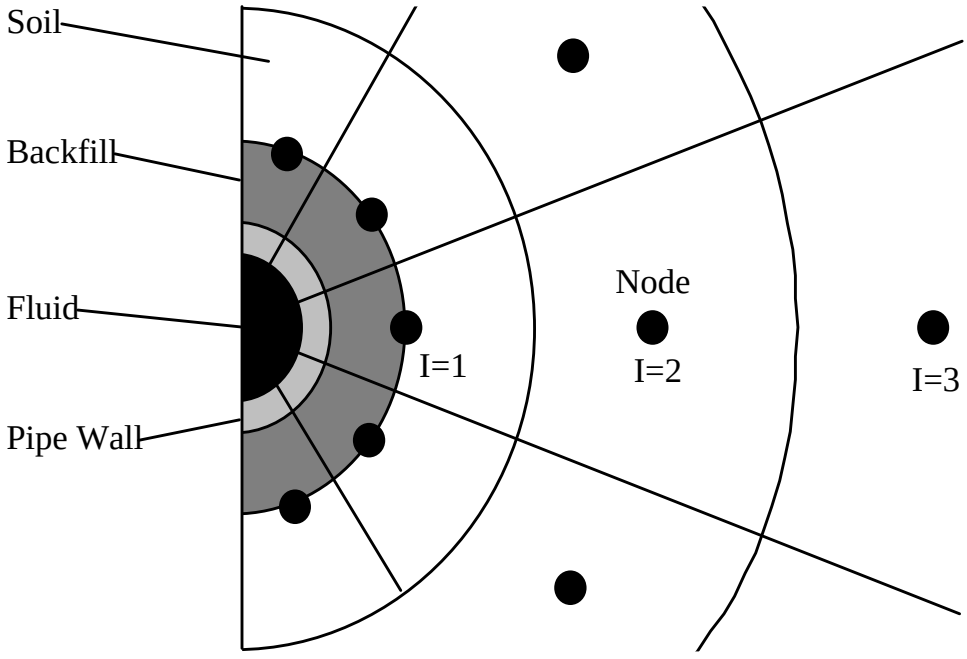

Figure 4.6 New model for heat transfer around pipe

the fluid to the first node, at i = 1, must pass through a thermal resistance that includes fluid forced convection, pipe wall, and backfill. Energy flowing from i=1 to i=2 must pass through the resistance which the small portion of soil provides. Using this new approach, the critical time step has been increased from 0.05 minutes to between 0.5 to 3 minutes, depending on the radii chosen for the innermost nodes.

The energy transfer to and from a fluid node was modeled as shown in the following figure, Figure 4.7, where U(j,k) is the fluid node temperature.

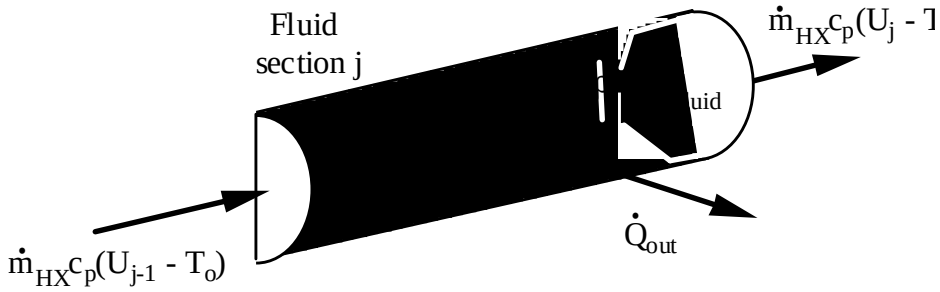

Figure 4.7 Energy diagram of fluid node

Equation 4.9 is used to model the energy transfer shown in Figure 4.7.

$$U(j,k+1) = U(j,k) + \frac{\dot{m}_{HX}dt}{(\rho V)_{fluid}}\left(U(j-1,k) - U(j,k)\right) - \frac{dt}{(\rho V c_p)_{fluid}}\dot{Q}_{out} \qquad (4.9)$$

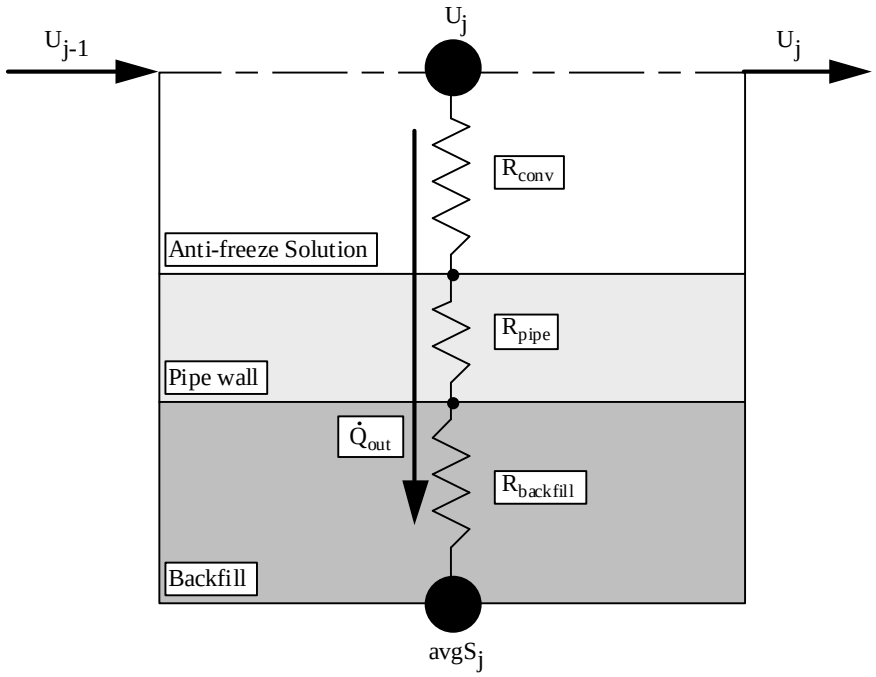

Figure 4.8 Model of heat transfer from fluid in section J

The energy flowing from the fluid into the soil, $\dot{Q}_{out}$, is calculated using the resistance network shown in Figure 4.8.

The resistance values shown in Figure 4.8 are calculated using equations 4.10, 4.11, and 4.12.

$$R_{fluid} = \frac{1}{h_{conv} A_{surface}} \tag{4.10}$$

$$R_{pipe} = \frac{\ln\left(r_{pipe,outer} / r_{pipe,inner}\right)}{\pi \, k_{pipe} \, \Delta Z} \tag{4.11}$$

$$R_{backfill} = \frac{\ln\left(r_{backfill,outer} / r_{backfill,inner}\right)}{\pi \, k_{backfill} \, \Delta Z} \tag{4.12}$$

Equation 4.13 shows how these resistance values are used to find $\dot{Q}_{out}$.

$$\dot{Q}_{out} = \frac{\left(U(j,k) - avgS_j\right)}{R_{totflow}} \tag{4.13}$$

where

$$R_{totflow} = R_{fluid} + R_{pipe} + R_{backfill} \tag{4.14}$$

and

$$\text{avg}S_j = \frac{\sum_{m=1}^{m_{max}} S(1, j, m, k)}{m_{max}} = \text{average temperature of inner soil ring.} \quad (4.15)$$

The convective resistance, R_{fluid}, is calculated as shown in equation 4.10. The ORNL paper proved through numerous tests that the heat transfer from the fluid to the soil is a weak function of the convection coefficient, and therefore an exact value of h_{conv} is not important for an accurate solution. The same conclusion can be drawn simply be comparing the relative values of the resistances effecting the heat transfer from the fluid to the soil. Some typical values of resistance are:

$$R_{fluid} = 0.05 \ \frac{\text{ÞF}}{\left(\text{Btu}/\text{min}\right)} \quad (4.16)$$

$$R_{pipe} = 0.75 \ \frac{\text{ÞF}}{\left(\text{Btu}/\text{min}\right)} \quad (4.17)$$

$$R_{backfill} = 0.65 \ \frac{\text{ÞF}}{\left(\text{Btu}/\text{min}\right)} \quad (4.18)$$

When flow is turbulent, the resistance due to convection accounts for less than 5% of the total resistance. As long as the fluid remains turbulent, R_{fluid} is not a significant contributor to the overall resistance. The thermal resistance of laminar flow has a value approximately equal to the resistance of the pipe wall causing laminar flow to significantly decrease the effectiveness of the buried heat exchanger. Turbulent flow is always maintained in ground heat exchangers for this reason.

The time step chosen for the TRNSYS simulation may not always be adequate for the ground heat exchanger model. TRNSYS users may set the simulation time step, dt_{TRNSYS}, from minutes to hours. Since the finite difference model must operate at a time step below the critical time step, usually in the range of 0.5 minutes to 3 minutes, the model is designed to

run at a user specified time step, DTIME, which is always less than or equal dt_{TRNSYS}. When TRNSYS calls the ground heat exchanger for an EWT, the ground heat exchanger subroutine will update node temperatures a number of times before it returns an answer. This way, the heat exchanger subroutine can be operated at time steps below the critical time step, while the simulation can operate at any time step desired. Three requirements must be satisfied when choosing a value of DTIME in order to assure correct operation of the ground heat exchanger model.

First, DTIME must be less than the amount of time it would take for a fluid front to flow through one section of pipe of length ΔZ. Equation 4.19 shows this calculation.

$$\text{DTIME}_{MAX} < \frac{\Delta Z}{\text{VEL}_{fluid}} \tag{4.19}$$

DTIME should be less than 25% of DTIME_{MAX} to avoid errors in the accuracy of the fluid energy balance.

The second requirement is that DTIME be an integer division of the simulation time step, dt_{TRNSYS}. The possible values of DTIME can be calculated using equation 4.20.

$$\text{DTIME} = \frac{dt_{TRNSYS}}{\text{integer}} \tag{4.20}$$

This means that when TRNSYS calls the ground loop model for a solution, the ground loop model takes an integer number of time steps to reach a solution. Since the ground heat exchanger time step is less than or equal to the simulation time step, several full grid temperature updates are made every simulation time step. With each grid temperature update, a value of the EWT is calculated. If dt_{TRNSYS} is 5.0 minutes and DTIME is 1.0 minute, there would be five grid wide updates, and five new EWT calculated. Since the program only returns one EWT per simulation time step, the average of these five EWT must be taken, as shown in equation 4.21.

$$EWT_{\text{simulation step}} = \frac{EWT_{(1)} + EWT_{(2)} + EWT_{(3)} + \ldots + EWT_{(\text{integer})}}{\text{integer}} \quad (4.21)$$

If dt_{TRNSYS} is not an integer multiple of DTIME, the averaging procedure will not operate correctly. The program could have been modified to handle non-integer situations, but it was much simpler to have the user input a DTIME which went into dt_{TRNSYS} an integer number of times.

The third requirement is that the ground loop time step be less than the critical time step. This is calculated using equation 4.4. The critical time step will either occur with the fluid node or with the first row of soil nodes. If all three of these requirements are met, the ground loop should run without experiencing instability or calculation errors.

4.7 Testing of the TRNSYS Buried Closed Loop Heat Exchanger

The TRNSYS model for the closed loop heat exchanger had to be tested. First, steady state runs were made and every node was checked to locate potential errors. Second, the transient behavior of the model was examined. The transient examination makes a comparison to another model, and plots the EWT vs. time for the entire year.

Three different tests were run to check the model reaction to steady state situations. First, the radial temperature profile was compared to that from an analytical solution. To analyze the radial heat transfer, the circumferential component was eliminated by removing any temperature gradients in the circumferential direction. This was accomplished by setting each of the farfield nodes to a constant temperature of 70°F. Fluid entered the pipe at a temperature of 30°F and a flowrate of 10 gallons per minute. When the temperature of the fluid leaving reached a steady value, the radial temperature profile of the soil region was compared to an analytical solution and matched up perfectly. This was expected since the resistance values were based on the same equation as the analytical solution.

Another steady state test was used to examine how the grid reacted when flow was stopped. This test was performed for a uniform farfield temperature of 70°F and also for a temperature profile given by the Kusuda ground temperature approximation in equation 4.5. For both runs, farfield conditions remained constant throughout the entire simulation, and initial soil nodes temperatures were 40 °F. With no flow, the grid with the 70°F boundary conditions became a uniform 70°F over the entire grid. For the model with the Kusuda approximation, the grid temperatures all approached the farfield temperatures for that depth, with some expected temperature distortions around the buried pipe.

After numerous steady state tests, all nodes were identified as working properly. There were no oddities discovered at the vertical line of symmetry, nor from section to section along the length of the pipe. The boundary conditions were found to be functioning properly.

Energy balances were performed locally on a node to node basis, as well as globally for the entire length of soil and pipe. Energy balances on each node showed correct operation, where the change in energy of each node equaled the difference of the energy entering and leaving the node. For the global energy balance, a simple two section system was monitored over one hour of operation. Energy flowing in from the farfield boundary was summed, as was the energy flowing into the first section and out of the second section. The change in temperature of every soil node and both fluid nodes was monitored to sum the total change in energy stored. Globally, the energy that entered from the farfield boundary plus the net energy carried by the flowing fluid equaled the change in energy of the entire grid of nodes.

The minimum EWT, which is the lowest water temperature entering the heat pump during the entire year, generated by the TRNSYS model was compared to commercial software used in the sizing of ground loops. In climates with large heating loads, ground heat exchangers are sized to provide fluid to the GCHP above a certain temperature during the worst winter conditions. This is done to protect the ground loop and heat pump equipment from damage

due to freezing coil fluid. Commercial programs use the line-source theory to predict ground loop lengths given a ground heat exchanger load, soil properties, location, loop formation, and a desired minimum EWT. Oklahoma State University produces one of the line source theory based ground heat exchanger sizing programs. This program, Closed Loop Ground Source Design (CLGS), was obtained courtesy of Professor Jim Bose at OSU (OSU, 1989). Using this program, a comparison was made to the TRNSYS ground heat exchanger model using the test parameters of Table 4.2.

Table 4.2 Parameters used in the loop length vs. EWT comparison

Winter Design Temperature	0 ℉	(-18 ℃)
Winter Thermostat Setting	70 ℉	(21 ℃)
Design Heating Load	65000 Btu/hr	(19 kW)
Outer Pipe Diameter	1.9 in	(48.3 mm)
Inside Pipe Diameter	1.6 in	(40.6 mm)
Pipe Thermal Conductivity	0.226 Btu/hr/ft/℉	(0.391 W/m/℃)
Pipe Burial Depth	8 ft	(2.43 m)
Soil Annual Mean Temperature	49 ℉	(9.4 ℃)
Amplitude of Surface Soil Temperature	21 ℉	(11.7 ℃)
Phase Constant	41 days	(41 days)
Soil Thermal Diffusivity	0.050 ft^2/hr	(1.3 W/m/℃)
Soil Thermal Conductivity	2.00 Btu/hr/ft/℉	(3.46 W/m/℃)
Heat Pump Characteristics	2.83 ton 7 gpm	(9.95 kW) (0.441 kg/s)

CLGS was used to find the length that corresponded to a given minimum EWT. TRNSYS simulations were run for several different grid designs to examine how the choice of the parameters, such as the number of sections and the farfield radius, affected the output. The minimum EWT generated by TRNSYS was the lowest temperature attained during the course

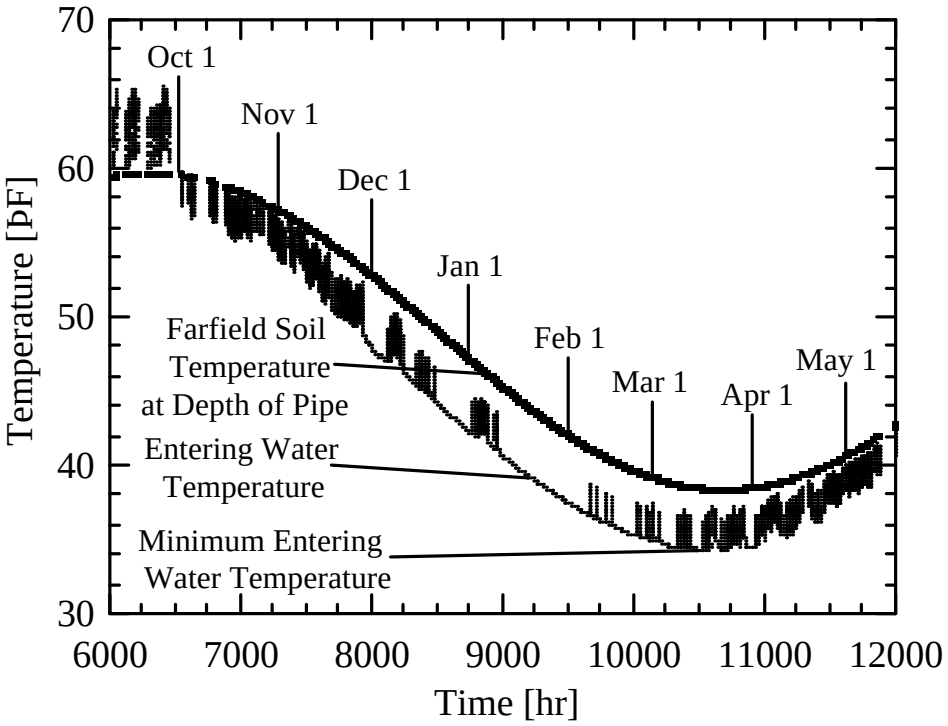

Figure 4.9 Entering water temperature vs. time of year

of an annual simulation. The graph in Figure 4.9 shows how the temperatures generated by the TRNSYS model vary with time of year. The EWT returned by the ground heat exchanger model is plotted for each TRNSYS time step for which there was GCHP operation. The minimum EWT, pointed out on the graph, typically occurs around the same time as the minimum soil temperature.

The results of this comparison are shown in Figures 4.10 and 4.11, and several trends are immediately noticeable. First, as the farfield radius of the TRNSYS model is increased, the results agree better with the CLGS output. Second, as the number of sections of the TRNSYS model is decreased, the results agree better with the CLGS output. Third, the TRNSYS model consistently predicts EWT which are higher than the CLGS program. These trends can be explained if one understands the models.

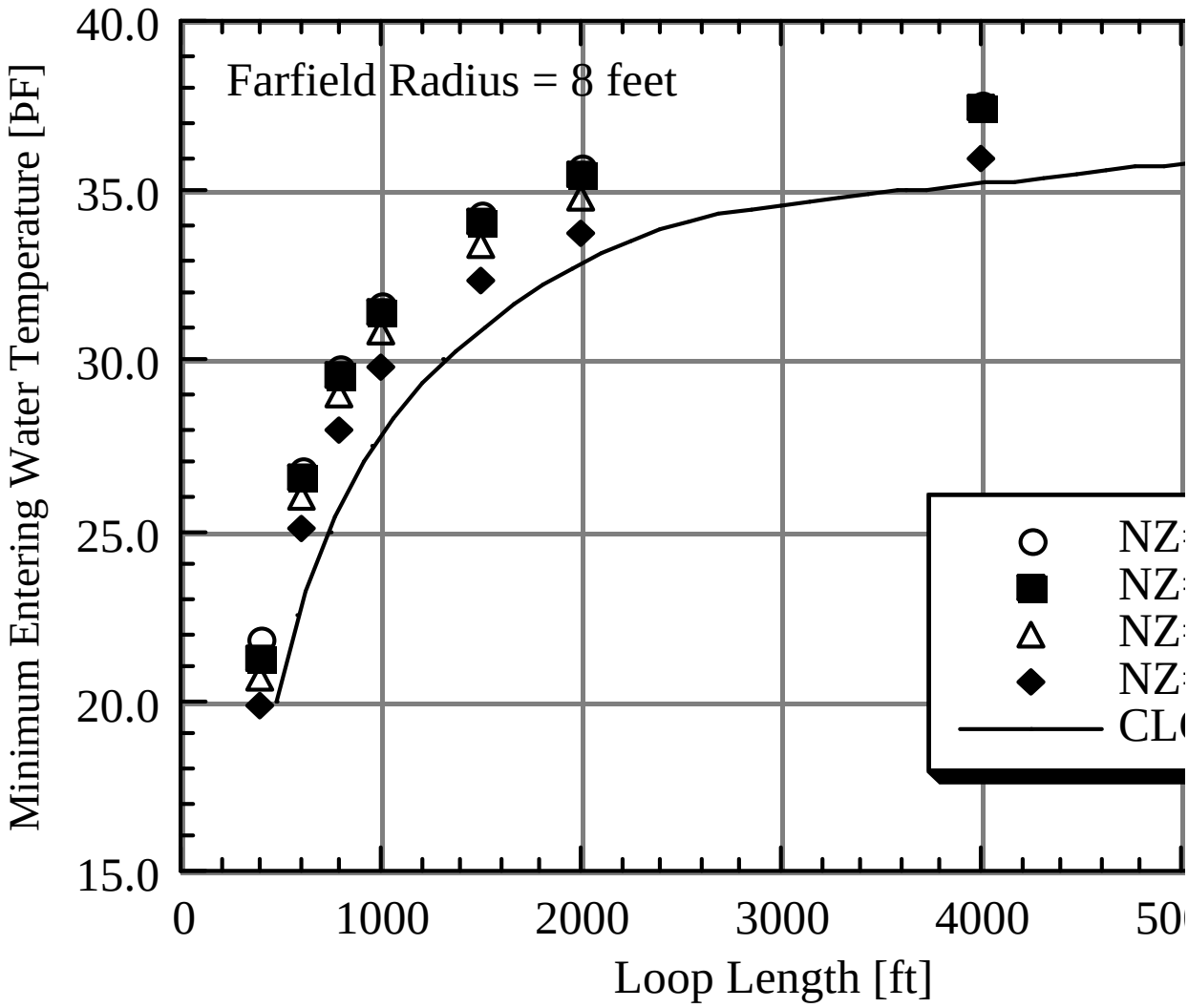

Figure 4.10 Comparison of CLGS and TRNSYS model

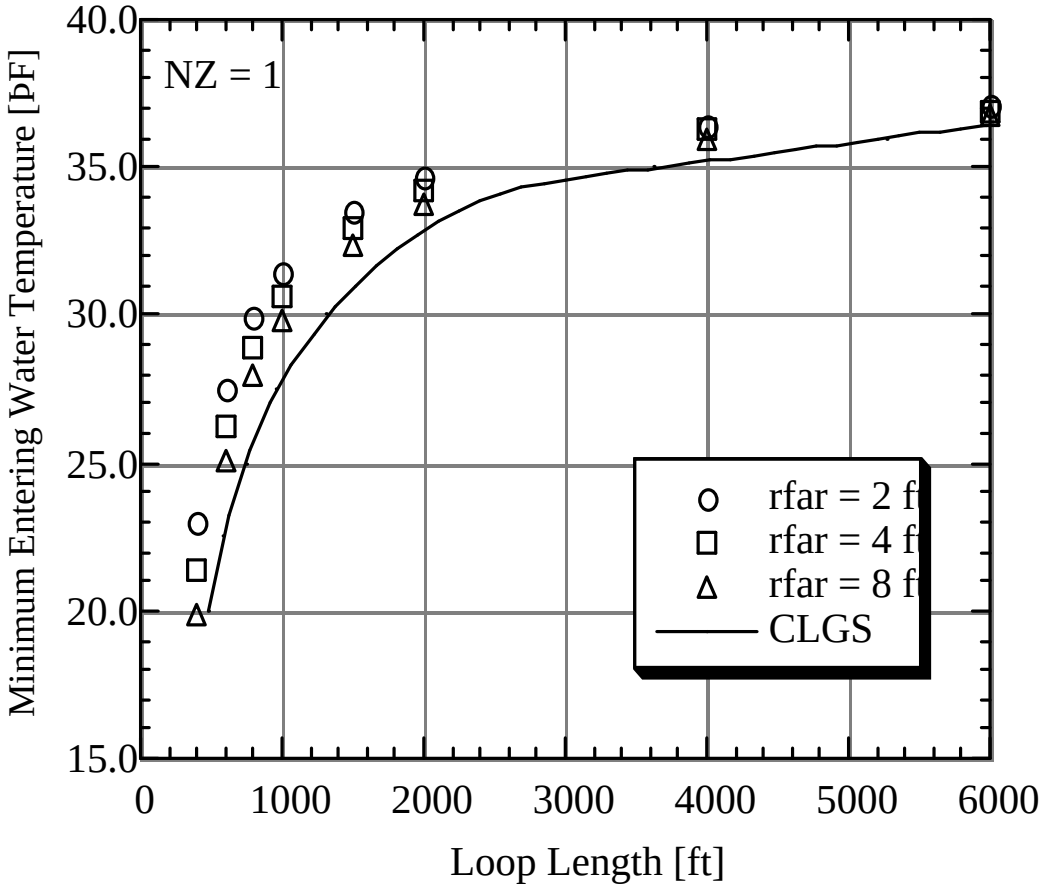

Figure 4.11 Comparison of CLGS and TRNSYS model

The line source theory assumes that a pipe is buried in a large cylinder of soil. The outer boundary of this cylinder is called the farfield radius, which is the distance from the pipe where the soil temperatures are undisturbed by the absorption and rejection of energy. With the line-source theory, the cylinder radius increases as the operating time of the buried pipe increases. This occurs because the energy stored in the cylinder of soil is removed by the heat exchanger faster than it can be replenished in by the surrounding soil, so temperatures decrease. It is assumed that the buried pipe has a uniform flux along its entire surface, and that there are no temperature gradients in the axial direction of the pipe (Hart, 1986), spreading the pipe load evenly over the entire length. Therefore, the end of the cylinder located near the fluid inlet experiences the same load as the outlet end of the cylinder. Figure

4.12 shows the line source modeling assumptions. The TRNSYS model divides the length into sections, where within each section there is uniform energy flux and no axial temperature gradients. However, the load is not evenly distributed over the entire length of the pipe, with the first nodes experiencing the largest loads.

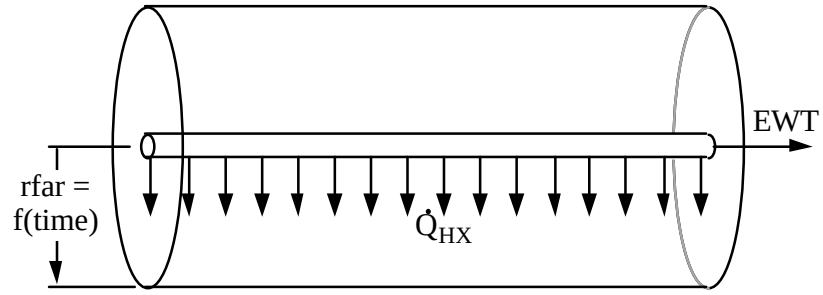

Figure 4.12 Line source theory assumptions

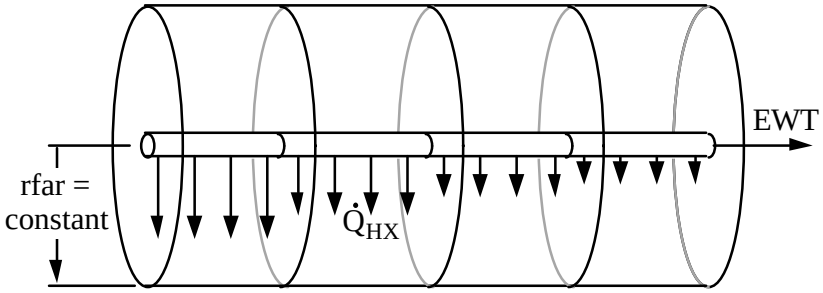

Figure 4.13 TRNSYS model when NZ = 4

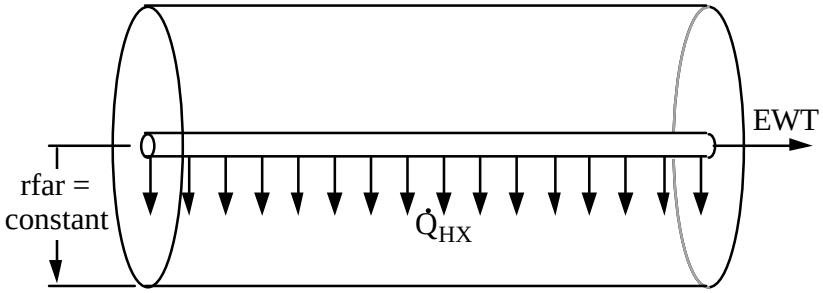

Figure 4.14 TRNSYS model when NZ = 1

The farfield radius is a fixed distance from the buried pipe, and has a maximum value equal to the pipe depth. Figure 4.13 shows this model. If the entire length of buried pipe is treated as one section, meaning NZ = 1, it would appear that the TRNSYS model was identical to the line source theory. Figure 4.14 shows how the TRNSYS model looks with only one section.

Figure 4.10 shows that the TRNSYS model, where the entire heat exchanger is treated as a single section, yields a higher EWT than the line source theory even though they are similar models. The difference is that the farfield radius of the TRNSYS model is a constant, whereas the line source theory farfield radius increases with operating time.

As a ground heat exchanger removes energy from the soil surrounding the buried pipe, the soil temperature around the pipe decreases, increasing the farfield radius. As more energy is removed from the ground, the farfield radius continues to increase. The effectiveness decreases because the temperature in the soil surrounding the pipe becomes lower, decreasing the temperature difference between the fluid and the surrounding soil. If the farfield temperature boundary is prevented from expanding beyond a certain point, as with the TRNSYS model, the rate of heat transfer is maintained artificially high, and the same length of pipe can deliver a higher EWT during the heating season. So, even when both models use only one section for the entire length of pipe, the TRNSYS model will return higher temperature. Figure 4.11 confirms the effect of the farfield radius, because as the farfield radius is moved in from 8 feet to 2 feet, the minimum EWT increases considerably.

Two factors contribute to the increase in EWT as the number of sections increases from 1 to 10 has two. The first factor is the proximity of the farfield radius, and the second factor is the distribution of the load over the length of the pipe.

The first factor, the location of the farfield radius, contributes in the following way. The first sections along the length of the pipe, nearest where the flow enters, experience the first demands for energy. With a real buried heat exchanger, when the first 100 feet of heat exchanger becomes cooled and its effectiveness declines, the greater part of the load is shifted along to the next section of pipe. This continues until the entire length of pipe is needed to deliver the desired minimum entering water temperature. The farfield radius of the TRNSYS model is limited by the burial depth of the pipe. As energy is removed from the

soil in the TRNSYS model, the temperature disturbance of the first section approaches its limited farfield radius, and its effectiveness reaches a steady value, higher than that section would experience if the farfield radius were allowed to increase. Thus, the first nodes meet more of the load than they should, requiring less of the load to be shifted to the next sections. The last sections along the pipe length are essentially not being used at all. This effect is most prominent when sections are shorter than 150 feet. In future models, this problem could be avoided by modifying the model to handle a farfield radius larger than the pipe depth. This would allow the effectiveness of the first sections to continue to decrease, thus shifting the load to the sections further along the pipe.

The second factor is a result the line-source theory assumption of a single section. It has been mentioned that the line-source theory makes conservative predictions, so that loop lengths are longer than needed (Hughes, 1985). This occurs because of the way the load is spread evenly over the entire length of pipe. If the pipe is broken into two sections, the minimum entering water temperature would increase. Figure 4.15 shows how this occurs.

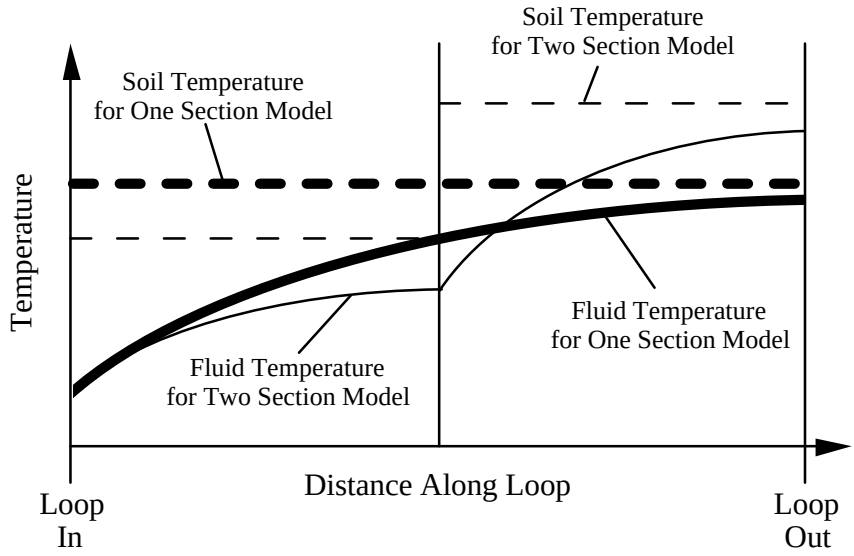

Figure 4.15 Fluid temperature profiles for one and two section loop models

With a single section, the entire length of soil decreases in temperature evenly. In a two section model, the first section is loaded more than the second section, bringing the soil around the first section to a lower temperature than that of the second section. The second section will have higher temperatures around it than it would if the entire length of the pipe were loaded evenly, which is shown by the dashed lines in Figure 4.15. This means that the outgoing fluid can reach higher temperatures with two sections than it could with one. So the fact that the TRNSYS model predicts higher temperatures is expected since it has many sections along the length of the pipe.

The bar graph in Figure 4.16 shows that the output is fairly insensitive to the parameters selected for the TRNSYS buried heat exchanger. The performance of the GCHP, although a function of EWT, is not a strong function. The small changes in EWT which result from the different model formations do not result in large changes in system energy consumption.

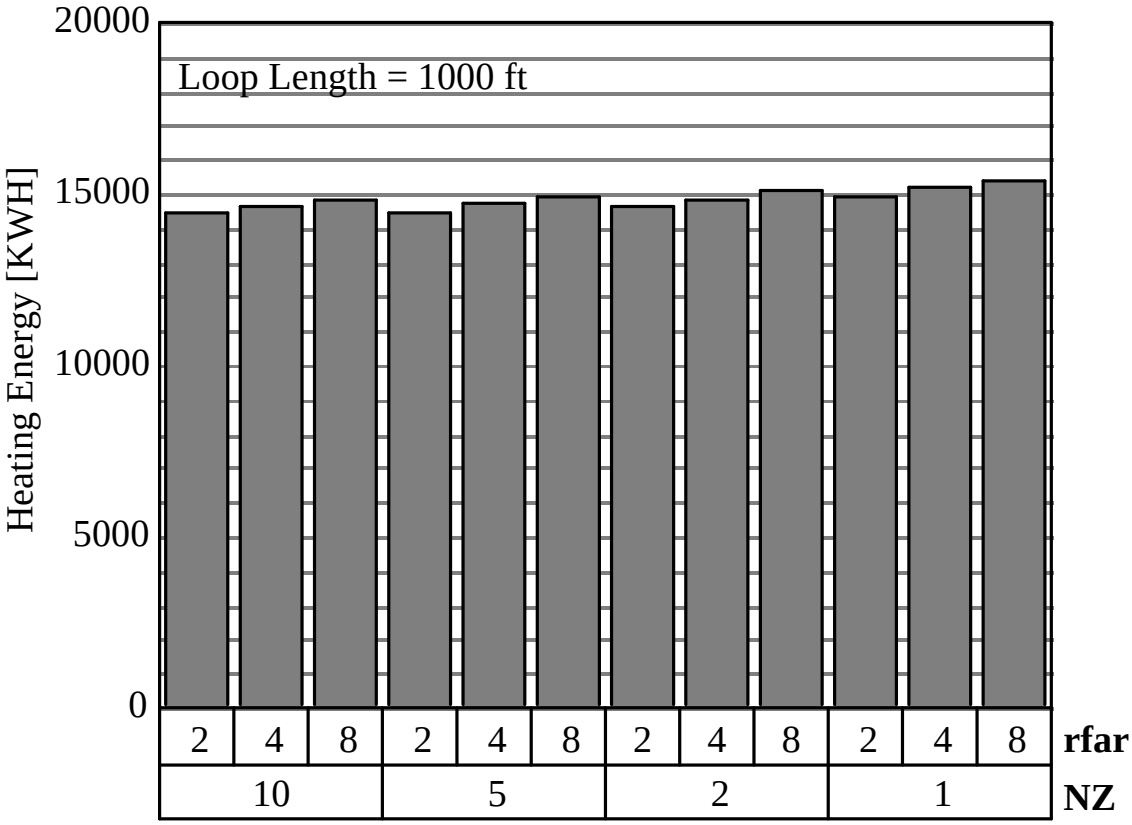

Figure 4.16 Heating energy required for a 1000 foot heat exchanger for combinations of NZ and rfar

CHAPTER
FIVE

ECONOMIC ANALYSIS METHODOLOGY

A major obstacle keeping ground-coupled heat pumps from becoming the heating and cooling unit of choice is customer uncertainty with the technology and economic benefits. The home owner, perceiving GCHP as a new technology, and uncertain of the actual benefits, may be wary of installing a GCHP system. Adding greatly to the customers perceived risk is the high initial cost which makes GCHP a risk that customers are generally not willing to accept. Contractors have commented that customers are less willing to spend $10000 on a heat pump than they are on a new automobile, even though the heat pump could save them thousands of dollars over its lifetime. Filling the house with nice carpeting and furniture has a higher priority than upgrading the heating and cooling system (Eaglin, 1994). For GCHP to gain popularity, people and utilities need to understand the benefits of GCHP financially and environmentally. The results of the economic analyses may reduce some of the uncertainty and sense of risk that the home owners feel.

In the previous chapters, models that simulate house heating and cooling systems were discussed. This chapter discusses the economics that will be used to analyze the output produced by the system models. The first section discusses the economic analysis that is directed toward the customer, showing the life cycle savings (LCS) they could realize by installing a GCHP. The second section discusses the calculation of the savings that a GCHP system means to society through avoided costs. The third section discusses some of the assumptions for the costs of loop and unit installations, electricity, and natural gas.

5.1 Economic Analysis - P_1, P_2 Method for Life Cycle Savings

The financial savings that a system generates over its lifetime is calculated with an economic analysis. When installing a new system, there are two important factors to consider. The first factor is the differential cost, which is how much more the system will cost to install than an alternative system. The second factor is the energy savings that the system will provide over its lifetime compared to an alternative system. An economic analysis is used to financially compare the systems, bringing the future differential costs and savings back to 1994 dollars. Many parameters are used in an economic analysis. The P_1, P_2 economic method combines all of the economic parameters into just two (Duffie, 1991).

The first parameter, P_1, is a function of the discount rate, fuel inflation rate, and the duration of the analysis. By multiplying the energy savings for one year of operation by P1, the total fuel savings the system represents over the analysis is brought back to 1994 dollars. Equation 5.1 shows the calculation of P_1.

$$P_1 = (1 - C\bar{t})\,PWF(N_e, i_F, d) \tag{5.1}$$

$$\begin{aligned} P_2 = {} & D + (1-D) * \frac{PWF(N_{min}, 0, d)}{PWF(N_L, 0, m)} \\ & - \bar{t}(1-D)\left[PWF(N_{min}, m, d)\left(m - \frac{1}{PWF(N_L, 0, m)} \right) \right. \\ & \qquad \left. + \frac{PWF(N_{min}, 0, d)}{PWF(N_L, 0, m)} \right] \\ & + M_S(1 - C\bar{t}) \times PWF(N_e, i, d) + tV(1 - \bar{t}) \times PWF(N_e, i, d) \\ & - \frac{C\bar{t}}{N_D} PWF(N'_{min}, 0, d) - \frac{R_v}{(1+d)^{N_e}} (1 - C\bar{t}) \end{aligned} \tag{5.2}$$

The second parameter, P_2, which is calculated as shown in equation 5.2, is multiplied by the differential cost of the installation. This calculates the 1994 dollar value of costs associated with operation, depreciation, taxation, installation, and loan payments. Both P_1 and P_2 bring

a series of future payments back to their present worth. This is done using the present worth factor for a series of payments shown in equation 5.3.

$$PWF(N,i,d)=\sum_{j=1}^{N}\frac{(1+i)^{j-1}}{(1+d)^{j}} \tag{5.3}$$

The LCS of a system can quickly be calculated for different values of P_1 and P_2 using equation 5.4.

$$LCS = P_1 * \Delta Cost_{operating} - P_2 * \Delta Cost_{installed} \tag{5.4}$$

The LCS realized by the homeowner is a trade off between initial costs and fuel savings. See the nomenclature section for a description of the parameters used in the calculation of P_1 and P_2.

The LCS calculation will be used with three different economic scenarios in this report. Five, ten, and twenty year analyses will be performed assuming 100% cash payment for the all system installations. Each analysis will assume the economic parameters shown in the Table 5.1 (WCDSR #2, 1994).

Table 5.1 Economic Parameters

Economic Parameter	Value
i	3.0 %
d	5.5 %
i_F	4.0 %
D	1.0
t_{bar}	25%
t	2.5%

The values of P_1 and P_2 are different for each system component due to differences in life expectancy and resale value. These values are listed for each system component in Table 5.2.

Table 5.2 Values of P_1 and P_2 used in the economic analyses

	P_2 Values		
	5 years	**10 years**	**20 years**
GCHP unit	0.365	0.660	1.095
Well Equipment	0.702	1.160	2.050
Closed Loop	0.556	0.952	1.438
ASHP unit	0.747	1.245	2.202
Air Conditioner	0.747	1.245	2.202
Gas Furnace	0.556	0.952	1.438
P_1 Values	4.6	8.9	16.6

5.2 Avoided Costs

When efforts are made to reduce the energy consumption and power of a system, society saves in many ways. Some of these savings are quantified by utilities as avoided costs in terms of three categories:

1) Energy (fuel)
2) Demand (capacity)
3) Externalities (emissions, environmental and public health)

The energy category accounts for the fuel that was saved as a result of the new system installation. Demand accounts for the reduction in peak kW draw resulting from the installation of the new system. This demand savings accounts for both costs associated with new generator construction and a reduction in the use of the less efficient peaking turbines. The third category, externalities, accounts for emissions such as SO_2 and greenhouse gases. This factor could either quantify the health effects these pollutants have on society, or they could be the costs incurred by the utility in controlling the emissions at the source. Although these values are often debated, they can help a utility rank the societal savings of a prospective technology and aid them in deriving an appropriate rebate.

Table 5.3 Avoided costs for peak demand and On/Off peak KWH usage.

Description/Time Period	Avoided Costs Including SO_2 Emissions	Avoided Costs Including SO_2 & Greenhouse Gas Emissions
Summer Peak Demand	72.67 $/kW-yr	72.67 $/kW-yr
Summer: on-peak	2.772 cents/KWH	4.471 cents/KWH
Summer: off-peak	1.767 cents/KWH	3.388 cents/KWH
Winter: on-peak	3.129 cents/KWH	4.796 cents/KWH
Winter: off-peak	2.187 cents/KWH	3.792 cents/KWH
Spring/Fall: on-peak	2.803 cents/KWH	4.420 cents/KWH
Spring/Fall: off-peak	1.937 cents/KWH	3.556 cents/KWH

Table 5.4 Seasonal on and off peak time periods

Time Period	Seasonal Months	Hours
Summer: on-peak	June through September	9 am to 9 pm - weekdays
Summer: off-peak	June through September	all other times
Winter: on-peak	December through March	9 am to 9 pm - weekdays
Winter: off-peak	December through March	all other times
Spring/Fall: on-peak	April, May, October, November	9 am to 9 pm - weekdays
Spring/Fall: off-peak	April, May, October, November	all other times

Wisconsin's Statewide Technical and Economic Potential (WCDSR #2, 1994), a part of the Public Service Commission's Advanced Plan 7, lists values for avoided costs for seasonal on and off peak values. Table 5.3, which was taken directly from the Advanced Plan 7, contains the avoided cost values used in this analysis. The values listed are average avoided costs that include most of the utilities in the state of Wisconsin. The first column of costs in the table considers SO_2 emissions, and the second considers SO_2 and greenhouse gas emissions. A description of the seasonal on and off peak time periods is shown in Table 5.4.

Avoided costs are calculated in the following way. Assume that for a new installation there is a choice between system A and system B. System A could be the original equipment or a conventional replacement. System B is the energy efficient alternative to system A. The energy saved for each period listed in Table 5.4 is calculated by subtracting the KWH used by system B during each period from the KWH used by system A during the same period. The avoided cost can be calculated for each of the time periods, as shown in equations 5.5 - 5.10.

$$AC_{sum,ON} = 0.02772\left[\frac{\$}{KWH}\right] * (KWH_{A,sum,ON} - KWH_{B,sum,ON}) \quad (5.5)$$

$$AC_{sum,OFF} = 0.01767\left[\frac{\$}{KWH}\right] * (KWH_{A,sum,OFF} - KWH_{B,sum,OFF}) \quad (5.6)$$

$$AC_{winter,ON} = 0.03129\left[\frac{\$}{KWH}\right] * (KWH_{A,winter,ON} - KWH_{B,winter,ON}) \quad (5.7)$$

$$AC_{winter,OFF} = 0.02187\left[\frac{\$}{KWH}\right] * (KWH_{A,winter,OFF} - KWH_{B,winter,OFF}) \quad (5.8)$$

$$AC_{spr/fall,ON} = 0.02803\left[\frac{\$}{KWH}\right] * (KWH_{A,spr/fall,ON} - KWH_{B,spr/fall,ON}) \quad (5.9)$$

$$AC_{spr/fall,OFF} = 0.01937\left[\frac{\$}{KWH}\right] * (KWH_{A,spr/fall,OFF} - KWH_{B,spr/fall,OFF}) \quad (5.10)$$

A summation of the avoided costs for each of the time periods, added to the avoided costs from to the reduced summer peak demand, is the avoided cost system B represents for one year of operation, as shown in equation 5.11.

$$\begin{aligned} AC_{TOTAL} = {} & AC_{summer\ Peak} \\ & + AC_{sum,ON} + AC_{sum,OFF} \\ & + AC_{winter,ON} + AC_{winter,OFF} \\ & + AC_{spr/fall,ON} + AC_{spr/fall,OFF} \end{aligned} \quad (5.11)$$

In order to determine the system lifetime avoided costs (LAC), the present worth factor in equation 5.3 will be used to bring future annual avoided costs back to current dollars. This calculation is shown in equation 5.12.

$$LAC = AC * PWF(N, i, d) \quad (5.12)$$

This project investigated the avoided costs associated with an upgrade to a GCHP in order to

offer an alternative economic view point to the life cycle savings economic analysis. There are two trains of thought that need to be discussed in this report. The customer possibly decides in terms of life cycle savings (the higher the better), while the utility considers avoided costs (the higher the better). Often, a high LCS and a high LAC do not occur simultaneously since the systems that provide the highest energy savings are often the most expensive for the customer to install. For instance, some systems may save the homeowner a significant amount of money but reduce peak demand very little. Other systems may not save the homeowner money due to high initial costs, and yet provide large energy savings and kW peak reductions for the utility. The utility, which may want the high efficiency system installed, can improve the LCS by offering to offset some of the initial cost through a rebate or other financial incentive. The LCS for the customer is improved and the installation proceeds to the satisfaction of both parties. An evaluation of rebates will be considered.

5.3 Summer Peak Demand Approximations

An important component of avoided costs is the summer peak power. This is the power at which a system operates during the most extreme summer conditions. At these conditions, most residential and commercial air conditioning units will be operating at the same time, creating the highest power peak the utilities will see all year. Futher, peak power is often provided by a different, often less efficient, power source (gas turbines) than the base power. If a system can perform the same job with a reduction in peak power, it represents an avoided cost to the utilities.

For this project, the peak power for each system was needed to make a comparison to the base system peak so avoided costs could be calculated. Peak power values are difficult to take from the actual simulation output. Direct comparisons cannot be made of system peak demand for all of the systems simulated since, at a certain time of day, one system may be operating while another is idle. In practice, the peak power of a system is the average power

of a many systems for a 15 minute period, taking into account the cycling of many pieces of equipment and the chance that a certain number are operating simultaneously. Since this requires a large number of computer runs, it was necessary to make approximations for the peak power requirements.

Two methods were used to appoximate the summer peak demand. For the roughest approximation, the steady state peak power was taken directly from the equipment performance catalogs, assuming that at the peak time of day a system would be operating continuously. This approximation is accurate for a system which operates continuously during the peak time periods. For instance, the 2.83 ton GCHP has a cooling capacity of 25.6 MBtu/hr, while the maximum summer cooling load is 30.0 MBtu/hr. This system would operate continuously to during the peak period. The average peak demand of a large number

Table 5.5 System peak demand - steady state values

System	Peak Demand [kW]
5.83 ton GCHP	2.5
4.75 ton GCHP	1.9
3.75 ton GCHP	3.3
3.33 ton GCHP	2.7
2.83 ton GCHP	2.1
3.84 ton ASHP	4.2
3.43 ton ASHP	3.7
2.60 ton ASHP	3.1
3.50 ton AC	3.8

of these systems would be the same as a single system since they would all operate continuously. This is not a good approximation when the equipment capacity exceeds the cooling load, as with the 3.84 ton ASHP. This unit has a cooling capacity of 31.8 MBtu/hr, so in a house with a cooling load of 30 MBtu/hr it will only operate for 94% of the time. For

a large number of systems cycling on and off at different times, the average peak demand would be lower than the steady state value of 4.16 kW. The peaks reported for various systems is listed in Table 5.5.

The second appoximation for peak demand takes into account cycling of systems, either on and off or between low and high speeds. In this approximation, the runtime necessary for a system to meet the peak summer cooling load of 30 MBtu/hr was calculated. There were three scenarios to calculate.

1) System cooling capacity is smaller than the load.
2) System cooling capacity is larger than the load.
3) Cooling load falls in between the high and low cooling capacities of a two-speed unit.

The peaks calculated for this approximation should better reflect the average of a large number of houses. The peaks calculated with this method are listed in Table 5.6.

Table 5.6 System peak demand - values accounting for cycling

System	Peak Demand [kW]
5.83 ton GCHP	2.3
4.75 ton GCHP	2.3
3.75 ton GCHP	2.1
3.33 ton GCHP	2.4
2.83 ton GCHP	2.1
3.84 ton ASHP	3.9
3.43 ton ASHP	3.7
2.60 ton ASHP	3.1
3.50 ton AC	3.8

Accounting for cycling shows that the summer peaks of the larger systems are competitive with the smaller systems. Since the larger systems are not operating for the entire hour, a

large number of systems will have a reduced average peak when compared to their steady state peak. The second approximation will be used since it provides a better comparison for the peaks of the large and small systems.

Values of cooling capacity and peak demand were needed from the performance catalogs to approximate peak demand. ASHP and air conditioners have performance that is a function of the ambient air temperature. For these systems, peak power was taken from the performance catalogs at an ambient air temperature of 95°F. This is approximately what the air temperature would be on a peak Wisconsin summer day. Total power includes the compressor, outdoor fan, and indoor circulating fan. GCHP would experience EWT of approximately 70°F when the cooling loads are largest. The appropriate cooling capacity and system power are taken from the performance catalogs. Total system power includes the compressor, indoor fan, and the pumping power for either the closed loop or well system.

One way in which a GCHP could reduce peak demand for a 15 minute period might include some contribution from the desuperheater. If the desuperheater meets most of the hot water load, the water tank resistive element does not need to operate for the entire 15 minute interval, reducing the average peak. This is a difficult peak reduction to pinpoint, being extremely unpredictable from household to household. So, no attempt was made to try to determine what the peak reduction was due to the desuperheater operation.

For system comparisons, winter peaks were approximated in a fashion similar to cooling. On the worst winter day, heating equipment loads can reach 60 MBtu/hr. Systems were assumed to be operating constantly for a 15 minute period, either at maximum capacity if the capacity of the equipment is lower than 60 MBtu/hr, or with just enough auxiliary to exactly meet the 60 MBtu/hr load. For instance, the electric baseboard heated house has 17 kW (58 MBtu/hr) of heat, so it was operating at maximum capacity. A large GCHP might meet 50 MBtu/hr of the load by itself at a power requirement of 5 kW, with the remaining 10 MBtu/hr being met

by exactly 2.93 kW of auxiliary heat, for a total power draw of 7.93 kW. EWT of 30°F were used for the GCHP, and an ambient air temperature of -20°F were used for the ASHP.

5.4 Energy, System, and Installation Costs

Before performing an economic analysis, costs of the equipment and energy must be determined. Many of the costs were readily available from contractors and manufacterers. However, often costs need to be approximated using what information is known. This section discusses the sources and assumptions that were used to find the costs.

The prices for the heating and cooling equipment are listed in Table 5.7. Prices for the GCHP unit, and the associated accessories, were given by a Water Furnace distributor in northern Indiana (Eaglin, 1994). These prices reflected approximately the average retail price a customer should expect to pay for that Waterfurnace model. Prices for the air conditioners, air-source heat pumps, and natural gas furnace were given by Jim Golish, a south eastern Wisconsin contractor (Golish, 1994). The extras listed in Table 5.7 are for the air handling unit and cooling coil associated with those pieces of equipment. Prices for the baseboard electric heaters were given by Fish Building Supply of Madison (Fish, 1994).

Installation prices shown in Table 5.8 were gathered from a number of sources. The installation of the air conditioners, natural gas furnace, electric baseboard heat, ASHP, and GCHP were given by Golish. These prices are what Golish thought to be typical estimates for the various unit installations. The GCHP installation is for the unit only, and does not include the installation costs associated with a buried heat exchanger. Estimates for the attachment of a well source to a GCHP were given by Lon Hoover of Illinois Geothermal Engineering, a GCHP supplier in northern Illinois. This attachment includes a water storage tank upgrade, a larger well pump, and if necessary, a newly drilled well. Ground heat exchangers installation costs, which are fairly complicated, are discussed in the following

paragraph.

Table 5.7 Heating and Cooling Equipment Costs

Equipment	Unit Cost	Auxiliary Heat	Desuper-heater	Extras
5.83 ton 2 speed GCHP Hi: 10.6 EER, 2.7 COP Lo: 17.1 EER, 4.0 COP	$5560	$310 for 15 kW	$350	none
4.75 ton 2 speed GCHP Hi: 12.6 EER, 3.0 COP Lo: 19.2 EER, 4.3 COP	$5170	$310 for 15 kW	$350	none
3.75 ton 2 speed GCHP Hi: 14.0 EER, 3.1 COP Lo: 20.1 EER, 4.3 COP	$4730	$310 for 15 kW	$350	none
3.33 ton 1 speed GCHP 15.2 EER, 3.4 COP	$4270	$310 for 15 kW	$350	none
2.83 ton 1 speed GCHP 14.4 EER, 3.3 COP	$3870	$250 for 10 kW	$350	none
3.84 ton ASHP 12 SEER	$2400	$300 for 20 kW	none	$500
3.43 ton ASHP 12 SEER	$2200	$300 for 20 kW	none	$500
2.60 ton ASHP 12 SEER	$1900	$300 for 20 kW	none	$500
3.5 ton Air Conditioner 12 SEER	$1650	none	none	$275
Natural Gas Furnace: eff = 96% , 60 MBtu/hr	$1500	none	none	none
Electric Baseboard Heater: 1.0 kW unit	$35	none	none	none

The ground heat exchanger installation, the major cost of the GCHP system, is also the most difficult to estimate. Each contractor uses a different loop formation and has to deal with different soil conditions. None of the contractors had determined what fraction of the installation cost was a fixed cost associated with moving equipment and preparing the site, and what variable costs were associated with trenching and laying pipe. However, contractors were able to provide a typical installation cost for their heat exchangers. Dan

Green, a GCHP contractor from Eau Claire, said that 90% of the loops installed by his company were from $2500 - $3000 for a 3 to 3.5 ton system (Green, 1994). Lon Hoover said that the loops installed in that area ran about $800 to $1000 per nominal ton. Loops in northern Indiana, which are shorter due to the milder weather, tended to cost between $2000 to $2500. The loop should cost from $2500 to $3000 for a 3.0 ton system.

Table 5.8 Heating and Cooling Equipment Installation Costs

Equipment	**Installation Cost**
Ground-Coupled Heat Pump	$1000 + $100 for Desuperheater
Air-Source Heat Pump	$1000
3.5 ton Air Conditioner	$500
Natural Gas Furnace	$500
Baseboard Electric Heat	$200
Existing Well Hook-up	$600
New Well Hook-up	$5500

An approximation was needed for the installation costs of the single pipe per trench model used the TRNSYS model. When loop lengths are varied in a LCS analysis, the installation cost of the longer or shorter loops will need to be accounted for. What makes this difficult is that the ground heat exchangers used in the field today are not single pipe per trench designs. In northern Indiana, the pipe arrangements have been parallel systems with six pipes per trench, with the pipes laid at 3.5 and 5.5 foot depths. Green uses an unusual buried heat exchanger formation, where three to six loops of pipe are placed at the bottom of a trench that is 8 feet wide by 8 feet deep. Hoover said that the typical pipe arrangement was a four pipe per trench parallel arrangement, with the pipes laid at 4 and 6 foot depths.

Steve Carlson, a principal engineer at CDH Energy Corp., has done some work on the

economics of GCHP (Carlson, 1994). Two different studies used an approach where the installation was broken into a fixed cost and a variable cost. In a national study the loop had a fixed cost of $1926 with a variable cost of $750/ton. In a north east utility study, the fixed cost was $1000 with a variable cost of $1000/ton. Both of these give an installation cost of around $4000 for a three ton GCHP. This is high considering the quotes provided for the area, but can be used as a guideline. Considering the information provided by contractors, the following approximation, in equation 5.13, will be used in this report to find the ground heat exchanger installation costs for Eau Claire. Equation 5.14 will be used for Madison.

$$C_{\text{Loop Installation}} = \$1200 + \frac{\$1}{\text{foot of trench}} \tag{5.13}$$

$$C_{\text{Loop Installation}} = \$900 + \frac{\$1}{\text{foot of trench}} \tag{5.14}$$

For the lengths used in the models, these equations provide loop installation costs of $2650 and $2800 for a 3.33 ton GCHP in Madison and Eau Claire, respectively.

The next cost that was needed for the economic analyses was that of energy, both electrical and natural gas. The competitiveness of GCHP against natural gas furnaces in the future depends entirely on the relative values of electricity and natural gas. If natural gas increases in price, GCHP will become an alternative. If natural gas experiences a price decrease, the GCHP loses the economic comparison. Currently, most electric rates are between $0.065 and $0.075/KWH, so a reasonable rate of $0.070/KWH will be used in this report. Natural gas prices are between $0.55 and $0.65/therm, so a value of $0.60/therm will be used for natural gas.

CHAPTER
SIX

RESULTS

This chapter presents the results from the TRNSYS simulations. Performance, life cycle savings, avoided costs, and general trends are discussed for the different sections of the analysis. The sections include an investigation of different systems for the same house in Madison and Eau Claire, an investigation of house size on the relative performance of several systems, and an investigation of life cycle savings for different heat exchanger lengths. Detailed listings of the parameters used for the systems in each of the above comparisons are in Appendix E (Madison), Appendix F (Eau Claire), Appendix G (House Sizes), and Appendix H (Heat Exchanger Lengths).

6.1 Heating and Cooling Systems in Madison

This investigation compared the energy consumption, peak heating and cooling power, avoided costs, and life cycle savings of GCHP, ASHP, resistance heat with an air conditioner, and a natural gas furnace with an air conditioner for a 50000 Btu/hr house in Madison. The GCHP equipment included two-speed compressor units of 5.83, 4.75, and 3.75 tons, and one-speed compressor units of 3.33 and 2.83 tons. These GCHP were used with a horizontal closed loop and a well source. The closed loop systems had one set with the desuperheater option and one set without, and the well source heat pumps all were equipped with desuperheaters. The ASHP units included one-speed compressor units of 3.84, 3.43, and 2.60 tons. The electrical resistance heated house had 17 kW of resistance elements and was

equipped with a 3.5 ton air conditioner. The natural gas heated house had a 58000 Btu/hr furnace with a 3.5 ton air conditioner. All systems used in this comparison were representative of the highest efficiency units on the market.

Graphs of the output from this analysis are contained in Appendix A. Figure A.1 shows the energy consumption of each system as a stack plot of heating, auxiliary heating, cooling, pumping, and hot water tank heating. Figure A.2 contains approximate summer and winter peak power for each system. Figures A.3 through A.40 show system energy consumption broken into monthly and seasonal ON/OFF peak periods. Figure A.41 shows approximate avoided costs for each system, compared to the base case of resistance heat with 3.5 ton air conditioner. Figures A.42 through A.44 show the life cycle savings of the systems for 5, 10 and 20 year periods. Figure A.45 shows the life cycle savings of 3.33 and 4.75 ton GCHP systems for different loop installation costs.

6.1.1 Comparison of System Energy Requirements

Figure A.1 shows the energy requirements of each system simulated in Madison. It can be seen that all water source heat pumps always used less energy than air source heat pumps and resistance heat. This improvement is due to the higher COP and capacity of the GCHP units which results from the higher source temperatures during the heating season. Comparing the different sized GCHP, it is seen that parasitic power plays a major role in diminishing the savings expected from the larger heat pumps. The reduction in the use of auxiliary heat provided by the larger heat pumps is offset by increased well or closed-loop pumping costs. Well source heat pumps in particular have large parasitic power requirements, with pumping energy twice that of the closed loop systems. The high parasitic energy requirement diminishes much of the energy savings the beneficial temperature of the well water provides.

The desuperheater option saved significant amounts of energy, reducing energy consumption by an average of 1600 KWH a year per system, or about $110 annually. At that rate, the desuperheater, which costs an additional $350, should pay for itself in just over three years.

With all of the GCHP options, both closed loop and well source, the 5.83 ton GCHP consumed more energy than the 4.75 ton GCHP. The 5.83 ton GCHP saves energy by reducing the auxiliary load, but has increased parasitic power and lower efficiency. The parasitics of the 5.83 ton GCHP are higher than those of the 4.75 ton unit for both the closed loop and well system applications. The catalog lists the 5.83 ton unit with a COP of 2.7, while the 4.75 ton unit has a COP of 3.0. This means that if both the 5.83 and 4.75 ton GCHP were able to meet the heating load of the house without auxiliary, the 4.75 ton GCHP would use less energy. The models showed that the 4.75 ton GCHP will still use less energy even if some auxiliary is needed to meet the largest heating loads.

6.1.2 Comparison of System Peak Demand

Traditional air conditioners cause utilities difficulty on the hottest summer days when the utility load is peaking. On the hottest days many air conditioners are running simultaneously, and with the high ambient air temperatures, most air conditioners and ASHP are running at their lowest efficiency and highest power draw of the entire cooling season. For this reason, utilities may wish to attempt to find systems that could help reduce the summer cooling peak. GCHP, with their reasonable entering water temperatures throughout the cooling season, can provide a reduction in summer peak.

Figure A.2 shows the summer peaks for the various systems simulated for Madison. Accounting for cycling, the large GCHP have an average peak demand similar to the smaller units, all falling between 2.1 and 2.3 kW. The units which use the surrounding ambient air as a sink, both the ASHP and air conditioner, have peak demands from 3.1 to 3.9. This means

that the GCHP provide between 0.7 to 1.8 kW peak reduction compared to the air source units. This is due to the GCHP use of ground temperatures which provide better efficiency and higher cooling capacity.

Winter peak demand is important in some rural areas with many electric heating customers, however a large majority of utilities only experiences summer peaking problems. For comparisons sake, GCHP provide reduced winter peak demand. Figure A.2 shows that the winter peaks of the GCHP systems are the lowest since they rely on auxiliary heat the least. ASHP, which during extreme cold will often not even operate, revert to behaving like a resistance heat system, so the ASHP winter peaks are identical to the resistance heated house at 17 kW. The larger GCHP have peaks of about 8 or 9 kW, while the smaller GCHP have peaks of about 12 kW.

6.1.3 Monthly Load Distribution

Figures A.3 through A.40 are included so that trends, such as reduced auxiliary operation, and energy distribution over the year can be easily viewed for each of the systems. It can be seen that while the cooling season provides a small energy savings, this savings is inconsequential compared to the energy savings that occurs during the heating season. The monthly graphs also allow trends such as pumping parasitics, auxiliary heat, and hot water tank energy to be tracked throughout the year. The figures with energy divided into seasonal on and off peak usage are included so that in the future one could use them in avoided cost calculations if needed.

6.1.4 System Avoided Costs

Avoided costs were calculated for each system in this comparison. Figure A.41, shows how GCHP and ASHP avoided costs compare to one another. There is not much variation between GCHP systems, since the energy savings from small to large is not substantial, and

peak demands are similar. GCHP provide avoided costs ranging from $580 to $650, while ASHP with their lower energy savings and inability to reduce peak demand have avoided costs of only $350. If ten years of avoided costs were brought back to present value, using a present worth factor of 8.53, a GCHP could generate about $5100.

6.1.5 Life Cycle Savings

A high life cycle savings motivates some customers into purchasing a system. The life cycle savings of the systems used in the Madison simulations are shown in figures A.42, A.43, and A.44 for 5, 10 and 20 year analyses, respectively. The base system, which will have a LCS of $0, is the resistance heated house with a 3.5 ton air conditioner. A natural gas furnace, against which GCHP cannot usually compete, has a LCS which is almost $5900 over a five year period, and $22600 over a 20 year period. This is compared to the best GCHP LCS of $3500 over 5 years and $15000 over 20 years for the 2.83 ton well source heat pump. This disparity between the LCS of the natural gas system and GCHP system is why currently GCHP are not considered competitive with natural gas.

Comparing ASHP with GCHP, it can be seen from figures A.42 to A.44 that all of the ASHP have higher LCS than the GCHP units. The low LCS of the GCHP systems is solely due to the high initial costs of equipment and installation, which ranges from $7500 to $11000 total. That is $3500 to $7000 more than any of the ASHP installations. The energy savings that GCHP generate is not great enough to overcome the large increase in initial costs.

The simulations reveal important trends with GCHP size and water source. Well source heat pumps, where an existing well can be upgraded, provides the highest LCS for each GCHP unit due to the lower initial cost. However, well source heat pumps, where a new well must be drilled, are always a losing investment. Smaller heat pumps have the largest life cycle savings, about $1500 to $2000 higher than the larger units for a 5 year period, and $4000 to

$5000 over a 20 year period. This is due to the high equipment and installation costs of the larger units.

Table 6.1 Effect of different energy costs on 10 year LCS

System	$0.065/KWH	$0.070/KWH	$0.075/KWH	$0.130/KWH
5.83 ton GCHP w/Desuperheater	$1602	$2630	$3658	$14964
4.75 ton GCHP w/Desuperheater	$2641	$3675	$4710	$16089
3.75 ton GCHP w/Desuperheater	$3267	$4270	$5274	$16311
3.33 ton GCHP w/Desuperheater	$3808	$4777	$5747	$16409
2.83 ton GCHP w/Desuperheater	$4371	$5296	$6221	$16392
5.83 ton GCHP	$1516	$2469	$3422	$13904
4.75 ton GCHP	$2603	$3566	$4529	$15127
3.75 ton GCHP	$3365	$4308	$5250	$15620
3.33 ton GCHP	$3689	$4581	$5472	$15284
2.83 ton GCHP	$4339	$5193	$6047	$15411
5.83 ton Well Sourced Heat Pump	$3453	$4482	$5510	$16823
4.75 ton Well Sourced Heat Pump	$4854	$5927	$7000	$18800
3.75 ton Well Sourced Heat Pump	$5597	$6655	$7713	$19356
3.33 ton Well Sourced Heat Pump	$6386	$7430	$8475	$19963
2.83 ton Well Sourced Heat Pump	$6730	$7726	$8722	$19679
3.84 ton ASHP	$7453	$8129	$8806	$16244
3.43 ton ASHP	$7101	$7728	$8356	$15260
2.60 ton ASHP	$6881	$7456	$8031	$14354
Natural Gas w/3.5 ton AC	$10264	$11818	$13372	$30465

If energy prices change, the economic advantages of the GCHP will change. For instance, using current installation costs, GCHP become competitive with ASHP when electricity costs are $0.13/KWH. Even for modest changes in the price of a KWH of electricity, the effect on the LCS of GCHP needed to be calculated. The effect of different energy prices on the system LCS are shown in Table 6.1 for a 10 year analysis. An increase of energy costs by $0.005/KWH causes an increase in ASHP 10 year LCS of about $600. The increase in 10

year LCS of the GCHP units is around $1000, so gap between the two closes as energy costs increase, as was expected.

For 3.33 and 4.75 ton GCHP systems, the effect of different loop installation costs on LCS was investigated. The results are plotted in Figure A.45. The results of this comparison show how higher installation costs for the same loop would effect the LCS of these systems. Increasing loop installation costs by $1000 will cost the customer $2500 over the equipment lifetime of 20 years.

6.1.6 Rebates Necessary for GCHP Systems to be Competitive

The main competition for GCHP systems is ASHP and natural gas heating. Due to the high initial cost of GCHP systems, utilities may offer a financial rebate to potential customers. This

Table 6.2 Rebates to make GCHP competitive with natural gas and ASHP systems over a 10 year period

GCHP system	Rebate for GCHP to be competitive with Natural Gas	Rebate for GCHP to be competitive with ASHP
5.83 ton Closed Loop	$5720	$3520
4.75 ton Closed Loop	$5080	$2980
3.75 ton Closed Loop	$4640	$2540
3.33 ton Closed Loop	$4280	$2130
2.83 ton Closed Loop	$3920	$1770
5.83 ton Well Source	$3520	$2020
4.75 ton Well Source	$2830	$1330
3.75 ton Well Source	$2490	$890
3.33 ton Well Source	$2130	$530
2.83 ton Well Source	$1970	$370

rebate needs to be enough for the GCHP to become economically competitive with the other conventional alternatives so that residential customers will install them. Rebates are listed in Table 6.2 for each of the GCHP systems installed in the Madison simulations that make the systems competitive with natural gas and ASHP units. For the most part, these rebates are lower than the avoided costs generated by the GCHP systems over a 10 year period.

6.2 Heating and Cooling Systems in Eau Claire

Further north in the state, winter ambient temperatures become colder on average. This leads to higher building loads and increased heating system run time. For both ASHP and GCHP, the larger building loads mean more auxiliary heat will be needed. ASHP begin to perform very poorly with the lower ambient temperatures and begin to rely increasingly on auxiliary heat. Ground temperatures also decrease, requiring an increased burial depth for ground heat exchangers, increasing installation costs.

This investigation compared the energy consumption, peak heating and cooling power, avoided costs, and life cycle savings of GCHP, ASHP, resistance heat with an air conditioner, and a natural gas furnace with an air conditioner for a 50000 Btu/hr house in Eau Claire. The equipment for Eau Claire was identical to that used in the Madison comparison, with the exception of the GCHP units investigated which were all equipped with desuperheaters. The comparisons assumed that equipment costs, installation costs, and energy costs were the same for Eau Claire as they were for Madison, making only a slight adjustment for the installation cost of the ground loop.

Graphs of the output from this analysis are contained in Appendix B. Figure B.1 shows the energy consumption of each system as a stack plot of heating, auxiliary heating, cooling, pumping, and hot water tank heating. Figure B.2 contains approximate summer and winter peak power for each system. Figures B.3 through B.30 show system energy consumption

broken into monthly and seasonal ON/OFF peak periods. Figure B.31 shows approximate avoided costs for each system, compared to the base case of resistance heat with 3.5 ton air conditioner. Figures B.32 through B.34 show the life cycle savings of the systems for 5, 10 and 20 year periods.

6.2.1 Comparison of Energy Consumption of GCHP and ASHP

Figure B.1 shows a comparison of annual system energy consumption for the Eau Claire systems. Eau Claire systems show the same general trends as the Madison systems, with all GCHP outperforming the ASHP, the 4.75 ton GCHP performing better than the 5.83 ton GCHP, and well source heat pumps performing the best overall. What is different is the amount by which the GCHP outperform the ASHP. The performance gap between the two systems increased, because while the GCHP source temperatures remain about the same, on average ambient air temperatures decrease. This means that the GCHP performed about the same, while the ASHP efficiency and capacity decrease. In Madison, the performance gap between the best ASHP and best closed loop GCHP was 8000 KWH. In Eau Claire, that gap has increased to 10300 KWH. This means that the LCS of the GCHP should be more competitive with the ASHP.

6.2.2 Avoided Costs

The peak demand used in the caluculation of avoided costs in Eau Claire are the same as those used in Madison. This is not a bad assumption since they both experience similar ambient temperatures on the peak summer days. In Eau Claire, where the performance advantages of the GCHP are more pronounced, they generate higher avoided costs than their Madison counterparts. Avoided costs, including only SO2 emissions, for the GCHP are up $80 to $100 compared to the Madison systems, whereas the avoided costs of the ASHP are about the same as those of Madison. This means that perhaps the utilities have slightly more

to gain from encouraging GCHP in northern regions than the utilities in the southern areas. The avoided costs for the Eau Claire systems are shown in Figure B.31.

6.2.3 Life Cycle Savings

Figures B.32 through B.34 show a comparison of the LCS of the Eau Claire systems. The GCHP have LCS that are more in line with being competitive with ASHP than they are in Madison. After 20 years, all of the GCHP system LCS are within $1000 or exceed the ASHP models. This is an improvement over the $3000 to $5000 gap that existed in the Madison comparison.

Table 6.3 Effect of different energy costs on 10 year LCS

System	$0.065/KWH	$0.070/KWH	$0.075/KWH	$0.110/KWH
5.83 ton GCHP w/Desuperheater	2991	4126	5261	13204
4.75 ton GCHP w/Desuperheater	4065	5209	6353	14362
3.75 ton GCHP w/Desuperheater	4402	5493	6584	14219
3.33 ton GCHP w/Desuperheater	4611	5642	6673	13891
2.83 ton GCHP w/Desuperheater	4938	5906	6874	13652
5.83 ton Well Sourced Heat Pump	4903	6043	7183	15163
4.75 ton Well Sourced Heat Pump	6313	7498	8683	16979
3.75 ton Well Sourced Heat Pump	6795	7946	9096	17151
3.33 ton Well Sourced Heat Pump	7623	8763	9902	17879
2.83 ton Well Sourced Heat Pump	7410	8459	9507	16846
3.84 ton ASHP	7571	8256	8942	13739
3.43 ton ASHP	7095	7722	8349	12739
2.60 ton ASHP	6800	7369	7937	11918
Natural Gas w/3.5 ton AC	11729	13457	15185	27282

The sensitivity of LCS to energy prices is examined in Table 6.3. Price changes of $0.005/KWH, and the $/KWH that makes GCHP competitive with ASHP after just 10 years is listed in the table. The small change in energy cost causes a $600 change in LCS for the

ASHP, and a $1000 change in LCS for most of the GCHP. As energy costs increase, the GCHP becomes more competitive with ASHP.

6.3 Effect of House Size on Life Cycle Savings and Avoided Costs

This analysis compared the performance, life cycle savings, and avoided costs of a 5.83 and 3.75 ton GCHP with desuperheater, a 3.84 ton ASHP, and resistance heat with 3.5 ton air conditioner in houses of 40000, 50000 and 60000 Btu/hr design heating loads. The goal was to evaluate whether certain equipment sizes had any advantages in certain house sizes.

Graphs of the output from this analysis are contained in Appendix C. Figure C.1 shows the energy consumption of each system as a stack plot of heating, auxiliary heating, cooling, pumping, and hot water tank heating. Figure C.2 contains approximate summer and winter peak power for each system. Figures C.3 through C.26 show system energy consumption broken into monthly and seasonal ON/OFF peak periods. Figure C.27 shows approximate avoided costs for each system, compared to the base case of resistance heat with 3.5 ton air conditioner. Figures C.28 through C.30 show the life cycle savings of the systems for 5, 10 and 20 year periods.

6.3.1 Ground Coupled Heat Pump Size and House Size

Figure C.1 shows annual energy consumption of the different systems in three different house sizes. In the smallest house size, a winter design load of 40000 Btu/hr, the 5.83 ton GCHP does not perform as well as the 3.75 ton GCHP. As mentioned in section 6.1.1, the COP of the 5.83 ton GCHP is lower than the COP of the 3.75 ton GCHP, and the 3.75 ton GCHP does not use enough auxiliary heat to reduce its overall COP to one which is below the 5.83 ton unit. Plus, the larger unit also has higher parasitics associated with greater pumping demands. In the 50000 and 60000 Btu/hr houses, the larger unit begins to perform better than the smaller unit, although just barely. This analysis suggests that installing a larger system to

eliminate auxiliary heat will not always reduce energy consumption. Larger systems have higher parasitic energy requirements as well as lower efficiency.

6.3.2 Peak Demand and Avoided Costs

The peak power draws for this comparison are shown in Figure C.2. Both summer and winter operation use the averaged power draw method discussed in chapter 5. GCHP consistently have summer peak demands that are lower than the air conditioner and ASHP. Winter peaks are also reduced with the GCHP unit for each house size.

Figure C.27 compares the avoided costs for the various systems. For each house size the GCHP provide $550 to $650 in avoided costs annually considering SO_2 emissions only. That is $250 to $300 more than the ASHP unit in each house size. It appears that even in a smaller house size the GCHP still provide superior performance to the ASHP.

6.3.3 Life Cycle Savings

For the LCS graphs of Figures C.28, C.29, and C.30, the LCS of the GCHP improves as the unit is decreased in size. Again, this is due to the lower initial costs of the entire system with lower tonnage GCHP. The LCS gap between the two GCHP systems closes as the house size increases. In the smallest house the gap is $1200 after 5 years. In the middle house the gap is $950, and in the largest house the gap has been reduced to $775. This makes sense, since the smaller GCHP will eventually be using significantly more auxiliary heat than the larger system.

6.4 Effect of Loop Length on GCHP Performance and LCS

In ground-coupled heat pumps, the performance varies with the length of the buried heat exchanger loop. If the coil is longer, the COP and EER will increase due to more reasonable

entering water temperatures, but the owner pays for higher installation costs and increased parasitics. Shorter coils will cost less to install and require less pumping work at the sacrifice of system performance. This analysis will compare the performance and LCS that a 3.33 ton GCHP with a desuperheater will experience with heat exchangers of different lengths. The investigation will consider different loop installation costs of $0.50, $1.00, and $2.00 per foot of trench with a fixed cost of $900.

Graphs of the output from this analysis are contained in Appendix D. Figure D.1 shows the energy consumption of the 3.33 ton GCHP with different heat exchanger lengths as a stack plot of heating, auxiliary heating, cooling, pumping, and hot water tank heating. Figure D.2 contains approximate summer and winter peak power for each length. Figures D.3 through D.14 show system energy consumption broken into monthly and seasonal ON/OFF peak periods. Figure D.15 shows approximate avoided costs for each length, compared to the base case of resistance heat with 3.5 ton air conditioner. Figures D.16 through D.18 are plots of the life cycle savings vs. loop length for the 3.33 ton GCHP, again with respect to a resistance heater with 3.5 ton air conditioner.

6.4.1 System Performance with Increasing Heat Exchanger Length

Increasing heat exchanger length improves GCHP performance by elevating the water temperature entering the GCHP. Figure D.1 shows how total system energy changes as heat exchanger length is increased. The trend of total energy consumed is downward with decreased returns for each addition to the length. For instance, from 1000 to 2000 feet the energy improvement is 1480 KWH, but for 2000 to 3000 feet the improvement is only 290 KWH. Pumping parasitics contribute to the decreased returns, since a longer pipe length has a larger head loss. However, the main contributor to the decreasing returns is the difference in temperature between the fluid and the ground. There is a limiting temperature that the fluid could attain with an infinitely long heat exchanger, which is that of the earth at the pipe

depth. Additional sections of pipe increase the EWT, but each additional section results in less of an increase in EWT increase since the potential for increase becomes less and less.

A run was made where the EWT were set equal to the undisturbed soil temperature throughout the year, mimicking an infinitely long heat exchanger. The results are shown in the following table, Table 6.4. The energy improvements made by increasing the heat exchanger length from 3000 feet to infinity are not great. There is an improvement of only 790 KWH when pumping energy is not included. So, parasitics aside, there is not much incentive to install loops of extraordinary dimension.

Table 6.4 Comparison of energy consumption of 3.33 ton GCHP with different loop lengths

Energy Requirements	1000 foot Loop	2000 foot Loop	3000 foot Loop	Infinitely Long Loop
Heat Pump Heating	7680	7390	7280	7100
Auxiliary Heat	3220	2010	1640	1130
Heat Pump Cooling	1200	1080	1049	1020
Hot Water Tank	4640	4480	4400	4330
TOTAL of above	**16740**	**14960**	**14369**	**13580**
Pumping	690	980	1280	??????

6.4.2 Life Cycle Savings vs. Heat Exchanger Length

Installation costs of buried heat exchangers are a function of heat exchanger length, as discussed in section 5.3. As discussed in section 6.4.1, the performance is also a function of heat exchanger length. The question is whether the GCHP performance improves enough to justify the expense of the longer lengths? Figures D.16, D.17, and D.18 are plots of LCS vs. Heat Exchanger Length for the 3.33 ton GCHP system used in this analysis. For several costs per length, the LCS decreases as length increases. The plots shows that for both expensive and inexpensive loop installations, the best LCS is consistently provided by the shortest

loops. With this heat pump, the loop length of 1500 feet produced a minimum entering water temperature of 24.2°F.

The limiting factor on how short a buried heat exchanger can be is the minimum entering water temperature. For instance, in this example of the 3.33 ton GCHP, the minimum length the heat exchanger could be was around 1000 feet, because below this the anti-freeze leaving the buried heat exchanger reached a temperature less than 20°F. This means that the fluid entering the heat exchanger is dangerously close to freezing. For this reason, the industry recommends never designing a ground loop to have water temperatures lower than 25°F (OSU, 1988). The GCHP used in this report were all designed to be near the maximum LCS, with minimum entering water temperatures within a degree of 25°F.

CHAPTER
SEVEN

CONCLUSIONS AND RECOMMENDATIONS

In this study, several residential heating and cooling systems have been modeled using the transient system simulation software, TRNSYS. The systems modeled include resistance heat, a natural gas furnace, a vapor-compression air conditioner, an air source heat pump, and a variety of ground source heat pumps. A finite difference model for a one pipe per trench closed-loop buried heat exchanger was created for use with the ground coupled heat pumps. Computer simulations were run comparing ground coupled heat pumps with the conventional heating alternatives. The output from the models was used to investigate the current economic position of GCHP in the residential heating and cooling industry.

7.1 Conclusions

One of the major accomplishments of this project was the design of transient analysis computer models for residential heating and cooling systems. These models will prove to be particularly useful for future GCHP energy analysis projects. As part of the GCHP model, a TRNSYS component for a single pipe per trench horizontal buried heat exchanger has been programmed using a finite difference approach. This component is a new addition to the TRNSYS library, since no previous heat transfer model for a buried pipe existed previously.

The models were used to find the economic viability of GCHP in Wisconsin, with simulations performed for Madison and Eau Claire. Installation and equipment costs obtained from contractors and manufacturers, performance output from the heating and

cooling system models, and a life cycle savings economic analysis were used to perform the economic comparison. Currently, GCHP provide better energy consumption than ASHP and resistance heating, with annual operating costs equal to a natural gas furnace with 3.5 ton air conditioner. However, the high initial cost of the GCHP systems reduces their life cycle savings considerably, causing them to be inferior choices for the residential customer.

The largest GCHP is not always the most efficient system for a given house size. Sizing a GCHP to meet all of the heating energy requirements, which means eliminating auxiliary heat, often does not ensure that the system will use less energy. A smaller heat pump which uses a small amount of auxiliary heat to meet the largest heating loads may have a higher average overall system COP than the larger system. Higher pumping parasitics and lower heat pump efficiency play roles in reducing the overall average COP of the larger GCHP systems.

Summer peak demand may play an important role in a utility encouraging the installation of a technology. An average peak demand for each unit was calculated by finding the runtime required by that unit to meet a 30 MBtu/hr sensible cooling load. Ground coupled units consistently provide from 0.7 to 1.8 kW reduction compared to the air source units.

Utilities that want to encourage GCHP installations will need to make them competitive in the residential heating and cooling market by offsetting some of the initial cost. Rebates were calculated that made GCHP competitive with ASHP and natural gas systems. Smaller GCHP systems required less of a rebate than the larger systems, and well source systems required lower rebates than closed loop systems due to the lower initial cost of the well system.

Encouraging the installation of large GCHP to reduce winter peak demand may be a good idea in a few regions, but for the most part utilities only need to reduce summer peak demand. Smaller GCHP units, with their lower installation costs, provide the customer with

significantly more LCS and still provide the same low peak demand during cooling. Utilities may find it easier to sell the public on the smaller units with lower installation costs and shorter loop lengths. Another advantage of the smaller systems is that smaller rebates make them competitive with conventional systems.

An important energy saving feature of the GCHP is the ability to heat water using a desuperheater. The energy savings a desuperheater generates was investigated for all of the heat pump models tested. The savings consistently totaled over $100 for each GCHP model. This is a significant savings since the desuperheater attachment costs only about $350 in addition to the GCHP unit.

7.2 Recommendations for Future Work

A key to modeling the performance of ground coupled heat pumps is the ground heat exchanger model. The current model represents an initial attempt at modeling the heat transfer and capacity in the soil around the pipe. However, as discussed in section 4.7, the model does have some limitations. The first limitation is the restriction on the distance of the farfield radius. Attempts should be made to design a model that does not have its farfield radius limited by the pipe depth. This would allow performance to degrade properly for each section as the temperature of the soil decreases with operation. The second limitation is that the one pipe per trench geometry is obsolete in ground coupled heat pump installations. Future work should concentrate on making models of multiple pipe per trench, as well as vertical heat exchanger designs. This would allow better direct comparisons to field monitored data to be made.

An important consideration for GCHP models is calculation speed. Since this model was programmed explicitly, small time steps were required to ensure calculation stability. This resulted in TRNSYS annual simulations that required 1.5 to 2.5 hours to complete on a work

station. In the future, in order to make GCHP modeling convenient for PC users, it would be a good idea to program the ground loop model implicitly to improve calculation speed.

In this project, the detrimental effects of heat pump and air conditioner cycling were not modeled. This was unfortunate since the transient analysis would be the perfect platform for such detailed modeling. The models could be improved by adding cycling effects that are either based on empirical data or based on current bin methods for cycling.

The desuperheater attachment to the ground coupled heat pumps is an advantage worth exploiting. The simple desuperheater set-up used in this project produced about $100 in energy savings annually, which is great considering it only costs $350. The TRNSYS model is ideal for investigating the energy savings of other possible arrangements, such as two tank designs and complicated control strategies. Current TRNSYS decks would simply need to be modified for different tank arrangements or controllers.

REFERENCES

ASHRAE. *1993 ASHRAE Handbook-Fundamentals*, Atlanta: American Society of Heating, Refrigerating and Air-Conditioning Engineers, Inc. pp 17.82-17.83, 1993.

Bryant Electric Air Conditioner: Model 597A - sizes 024 thru 060, Bryant Air Conditioning, Form No. PDS 597A.24.3B, 1991.

Carlson, Steve, personal communication, CDH Energy Corp., Cazenovia, NY, 1994.

Duffie, J. A., and Beckman, W. A., *Solar Engineering of Thermal Processes*, 2nd edition, John Wiley & Sons, New York, 1991.

Eaglin, Charlie, personal communication, Loopmaster, Inc., IN, 1994.

Electric Power Research Institute (EPRI). *WATSIM User's Manual Version 1.0*. October 1992.

Fish Building Supply, personal communication, Madison, WI, 1994.

Golish, Jim, personal communication, Jones Refrigeration, WI, 1994.

Green, Dan, personal communication, Water Source Heating & Cooling, Inc., Eau Claire, WI, 1994.

Hart, D.P., and R. Couvillion. *Earth-Coupled Heat Transfer*, Prepared for the National Water Well Association, Dublin, OH. 1986.

Hoover, Lon, personal communication, Illinois Geothermal Engineering, Russell, IL, 1994.

Hughes, P. J., et al, Residential Earth-Coupled Heat Pump Demonstration: Phase 1 and 2 Final Report, Report 85-20, New York State Energy Research and Development Authority (NYSERDA), Albany, NY, October 1985.

Klein, S.A., et al., TRNSYS - *A Transient System Simulation Program*, version 14.1, Solar Energy Laboratory, University of Wisconsin-Madison, Madison, WI, 1994.

Kusuda, T., and Archenbach, P. R. "Earth Temperature and Thermal Diffusivity at Selected Stations in the United States", ASHRAE Trans., Vol. 71, Part 1, 1965.

Lennox Industries, Inc. *Lennox Heat Pump Outdoor Units: 11.75 to 13.70 SEER*, Bulletin #210023, 1993.

Mei, V.C., "Horizontal Ground-Coil Heat Exchanger Theoretical and Experimental Analysis.", Oakridge National Laboratory/CON-193, December 1986.

Mei, V.C. "New Approach for Analysis of Ground-Coil Design for Applied Heat Pump Systems." ASHRAE Transactions, Vol. 91, Part 2. 1985.

Meyer, Denny, personal communication, WaterFurnace International, Indianapolis, IN, 1994.

Oklahoma State University, CLGS - *Closed-Loop/Ground-Source Heat Pump Design*. 1989.

Oklahoma State University. *Closed-Loop/Ground-Source Heat Pump Systems - Installation Guide*. Prepared for the National Rural Electric Cooperative Association and distributed by the International Ground-Source Heat Pump Association. 1988.

Temperature Systems, Inc., personal communication, Madison, WI, 1994.

U.S. Department of Energy, National Earth Comfort Program, *Geothermal Heat Pump Market Mobilization and Technology Demonstration* - A Proposal for an Industry-Government Collaborative, June 1994.

WaterFurnace, Dealer Manual, Desuperheater Pump Kit Installation Manual, 1990.

WaterFurnace Energy Analysis, Version 4.25. Indianapolis, IN: WaterFurnace International, Inc.

WaterFurnace Premire AT Series: Vertical and Horizontal Units 3/4 to 4 Tons, WaterFurnace International, Inc., Catalog no. WF438, 1992.

WaterFurnace Premire AT Series, Two-Speed: Vertical and Horizontal Units 4 to 6 Tons, WaterFurnace International, Inc., Catalog no. WF438, 1992.

Wisconsin Center for Demand Side Research, *An Assessment of Potential Heat Pump Applications in Wisconsin*, WCDSR INT-94001, 1994.

Wisconsin Center for Demand Side Research, *Wisconsin's Statewide Technical & Economic Potential*, WCDSR-119-1, 1994.